

1 **Protein visualization and manipulation in *Drosophila* through the use of epitope**
2 **tags recognized by nanobodies**

3
4 Jun Xu^{1, #, *}, Ah-Ram Kim^{1, #}, Ross W. Cheloha², Fabian A. Fischer², Joshua Shing
5 Shun Li¹, Yuan Feng¹, Emily Stoneburner¹, Richard Binari¹, Stephanie E. Mohr^{1, 3},
6 Jonathan Zirin^{1, 3}, Hidde Ploegh² and Norbert Perrimon^{1, 3, 4, 5, *}

7
8 ¹ Department of Genetics, Blavatnik Institute, Harvard Medical School, Boston,
9 Massachusetts, USA.

10 ² Boston Children's Hospital and Harvard Medical School, Boston, Massachusetts,
11 USA.

12 ³ Drosophila RNAi Screening Center, Harvard Medical School, Boston,
13 Massachusetts, USA.

14 ⁴ Howard Hughes Medical Institute, Boston, Massachusetts, USA.

15 ⁵ Lead Contact

16
17 # co-first authors

18
19 *Correspondence: Jun_Xu@hms.harvard.edu; perrimon@genetics.med.harvard.edu.
20
21

22 **Abstract**

23 Expansion of the available repertoire of reagents for visualization and manipulation of
24 proteins will help understand their function. Short epitope tags linked to proteins of
25 interest and recognized by existing binders such as nanobodies facilitate protein
26 studies by obviating the need to isolate new antibodies directed against them.
27 Nanobodies have several advantages over conventional antibodies, as they can be
28 expressed and used as tools for visualization and manipulation of proteins *in vivo*. Here,
29 we characterize two short (<15 aa) NanoTag epitopes, 127D01 and VHH05) and their
30 corresponding high-affinity nanobodies. We demonstrate their use in *Drosophila* for *in*
31 *vivo* protein detection and re-localization, direct and indirect immunofluorescence,
32 immunoblotting, and immunoprecipitation. We further show that CRISPR-mediated
33 gene targeting provides a straightforward approach to tagging endogenous proteins
34 with the NanoTags. Single copies of the NanoTags, regardless of their location, suffice
35 for detection. This versatile and validated toolbox of tags and nanobodies will serve as
36 a resource for a wide array of applications, including functional studies in *Drosophila*
37 and beyond.

38
39
40 **Introduction**

41 Conventional antibodies typically have a MW ~150-160 kDa and are composed of
42 four polypeptides, two identical heavy chains and two identical light chains. Size and
43 composition of conventional immunoglobulins impose limitations on their application
44 to *in vivo* studies. The recent development of smaller and single-polypeptide

1 recombinant protein binders, such as single chain variable fragments
2 (scFvs, ~25kDa), single-domain antibodies or 'nanobodies' (~12-15kDa), and
3 designed ankyrin repeat proteins (DARPs, 18 kDa for five repeats), has enabled
4 many new applications (*Harmansa and Affolter, 2018*). These new types of
5 recombinant binders are small and stable molecules that can be encoded in the
6 genomes of model organisms or cells. Moreover, the coding sequences of these
7 binders can be fused to various effector domains, making them useful as tools for
8 imaging and for regulating the function of target proteins of interest (POIs) *in*
9 *vivo* (*Helma et al., 2015; Harmansa and Affolter, 2018; Aguilar et al., 2019*). For
10 example, a protein binder fused to a fluorescent protein can be expressed *in vivo*,
11 where it can then bind to an endogenous target protein, an epitope-tagged protein, or
12 even a post-translational modification, thus allowing visualization of subcellular
13 localization of the target (*Harmansa and Affolter, 2018; Aguilar et al., 2019*). This is
14 not usually possible when using conventional antibodies, which fail to assemble in
15 the reducing environment of the cytosol.

16 Among available protein binders, camelid-derived nanobodies are particularly
17 useful, as they consist of a single monomeric variable antibody domain that is the
18 product of selection *in vivo*. Nanobodies are no less specific than conventional
19 antibodies. Given their small size, nanobodies are easy to express in *Escherichia*
20 *coli*, either alone or fused to a fluorescent marker or enzyme. The small size of
21 nanobodies also allows better super-resolution microscopy than antibody-based
22 imaging (*Fornasiero and Opazo 2015; Mikhaylova et al., 2015; Virant et al., 2018;*
23 *Fang et al., 2018*), and enables binding to epitopes not accessible to full-length
24 conventional antibodies. Because nanobodies are usually stable in the reducing
25 environment of intracellular space and are encoded as a single polypeptide,
26 nanobodies or nanobody fusion proteins can be expressed in eukaryotes and used
27 for a number of *in vivo* applications (*Helma et al., 2015*).

28 Nanobodies are powerful tools for manipulation of protein function and
29 localization, as has been illustrated using nanobodies against GFP. For example,
30 GFP-tagged proteins can be degraded using a GFP-targeting nanobody fused to an
31 E3 ligase component, an approach that has been used for studies in *Drosophila*
32 *melanogaster*, *Caenorhabditis elegans*, and *Danio rerio* (*Caussin et al., 2011;*
33 *Wang et al., 2017; Yamaguchi et al., 2019*). GFP-tagged proteins can be re-localized
34 using a GFP-targeting nanobody fused to sequences or domains that specify a
35 particular subcellular localization (*Harmansa et al., 2015; Harmansa et al., 2017*).
36 Many proteins in model organisms such as *Drosophila* have been tagged with GFP,
37 suggesting general applicability of the approach. However, the fusion of a target
38 protein with GFP is not necessarily compatible with all applications, a significant
39 limitation of a GFP-targeted approach. GFP is a bulky (27 kDa) substituent that might
40 affect function or localization of the tagged protein. In addition, maturation of the GFP
41 chromophore is slow, limiting its use for the imaging of nascent proteins.

42 An alternative approach would be to combine conventional epitope tags with the
43 advantages of nanobody-based targeting. Because of their small size, epitope tags
44 are less likely than GFP to interfere with the overall structure of the tagged protein.

1 Several nanobodies that recognize small epitope tags have been isolated, including
2 tags known as BC2-tag, EPEA-tag, MoonTag, and ALFA-tag (*Traenkle et al., 2015*;
3 *De Genst et al., 2010*; *Boersma et al., 2019*; *Tanenbaum et al., 2014*; *Götzke et al.,*
4 *2019*; *Cheloha et al., 2020*). Some of these have been used to visualize and
5 manipulate tagged proteins by changing their abundance or localization using tag-
6 targeting nanobodies in mammalian cells (*Zhao et al., 2019*; *Vigano et al., 2021*). The
7 recently developed ALFA nanobody (NbALFA) recognizes a short peptide of 13
8 amino acids and provides a system useful for immunoblotting, protein purification,
9 and imaging (fixed or live cells) (*Götzke et al., 2019*). In addition, it has been recently
10 reported that HA frankenbody, a single-chain variable fragment engineered from anti-
11 HA antibody, can be used for live imaging and protein degradation *in vivo* in
12 *Drosophila* (*Vigano et al., 2021*). However, to the best of our knowledge, short linear
13 epitope tag-specific nanobodies have yet to be applied for use *in vivo* in *Drosophila*
14 or other multicellular organisms.

15 To expand the repertoire of nanobody-recognized tags (NanoTags) and
16 corresponding nanobody tools, we characterized two NanoTags, VHH05- and
17 127D01-tags, and their corresponding nanobodies, NbVHH05 (*Ling et al., 2019*) and
18 Nb127D01, for cellular and *in vivo* studies in *Drosophila*. Both nanobodies can be
19 genetically encoded as fluorescent protein fusions (i.e., chromobodies, CBs) that
20 enable detection of target proteins that carry NanoTags at N-terminal, internal or C-
21 terminal sites. We show that these nanobodies are useful for multiplexed
22 immunostaining, immunoblotting, and immunoprecipitation. We show that
23 NanoTagged proteins can be manipulated by nanobodies fused to various
24 subcellular localization signals. Moreover, in transgenic flies that overexpress
25 NanoTagged proteins, we confirmed that the tagged proteins can be detected using
26 GFP-tagged nanobodies expressed *in vivo* (i.e. with CBs) or by immunostaining.
27 Finally, using CRISPR-based genome engineering, we generated flies with
28 NanoTags inserted into endogenous genes. Our data show that VHH05- and
29 127D01-tags and their corresponding nanobodies can be used effectively for labeling
30 and manipulating proteins, providing powerful tools for functional studies in
31 *Drosophila* and other organisms.

32

33 **Results**

34 **Characterization of VHH05 and 127D01 NanoTags**

35 We selected two nanobody/NanoTag pairs to test in *Drosophila*, NbVHH05/VHH05-
36 tag and Nb127D01/127D01-tag. NbVHH05 is a 111 amino acid (aa) nanobody that
37 recognizes a 14 aa sequence (VHH05-tag, QADQEAKELARQIS) derived from the
38 human E2 ubiquitin-conjugating enzyme UBC6e (**Figure 1A, B**), and has a binding
39 constant (K_d) for the VHH05-tag of ~0.15 nM (*Ling et al., 2019*). Nb127D01 is a 115
40 aa nanobody that binds to an extracellular portion of the human C-X-C chemokine
41 receptor type 2 (CXCR2) (*Bradley et al., 2015*). As the extracellular region of CXCR2
42 is large, we reduced the epitope-binding region to a minimal sequence of 10 aa
43 (127D01-tag, SFEDFWKGED) (**Figure 1C,D; Figure 1—figure supplement 1**) to
44 obtain a more versatile tag, and determined the K_d of Nb127D01 to this tag to be <50

1 nM (data not shown). Protein-protein BLAST searches with both NanoTags failed to
2 identify fully homologous sequences in the *Drosophila* proteome, thus reducing the
3 possibility of spurious cross-reactions with endogenous, untagged proteins.

4 To determine whether these NanoTags can be used for live imaging, we
5 visualized both the NanoTags and their corresponding nanobodies concurrently. To
6 do this, we constructed vectors that use the *Actin5c* promoter to ubiquitously express
7 mCherry proteins equipped with the NanoTags and with different cell compartment
8 localization sequences at the N-terminus: a cell membrane localization protein
9 (murine CD8 gene, NM_009857.1), a mitochondrial outer membrane sequence (TM
10 domain of *Homo sapiens* CDGSH iron sulfur domain 1, NM_018464.5), and a
11 nuclear localization sequence (histone H2B gene, NM_001032214.2). We also
12 constructed vectors that ubiquitously express GFP-tagged nanobodies (NbVHH05-
13 GFP and Nb127D01-GFP) (**Figure 1—figure supplement 2A,B**) under the control of
14 the *Actin5c* promoter.

15 When expressed alone in *Drosophila* S2R+ cells, NanoTagged mCherry fusion
16 proteins were observed in the expected subcellular compartments (**Figure 1—figure
17 supplement 2D**), indicating that the VHH05- and 127D01-tags do not affect protein
18 localization. When either NbVHH05-GFP or Nb127D01-GFP was expressed in cells,
19 we observed a GFP signal in the nucleus and the cytoplasm (**Figure 1—figure
20 supplement 2C**). Next, we co-transfected S2R+ cells with either mCherry-VHH05
21 fusion proteins and NbVHH05-GFP or mCherry-127D01 fusion proteins and
22 Nb127D01-GFP. In all cases, the GFP and mCherry signals colocalized and with a
23 distribution indistinguishable from that of mCherry fusions alone (**Figure 1—figure
24 supplement 2E,F**). We also tested whether mCherry-tagged nanobodies (NbVHH05-
25 mCherry or Nb127D01-mCherry) colocalized with mitochondrial GFP tagged with the
26 VHH05-tag or the 127D01-tag, respectively. As expected, we observed colocalization
27 of NbVHH05-mCherry and mito-GFP-VHH05 when expression vectors for each were
28 co-transfected in S2R+ cells (**Figure 1—figure supplement 2G**). Similarly,
29 Nb127D01-mCherry and mito-GFP-127D01 colocalized with mitochondria (**Figure
30 1—figure supplement 2H**).

31 We next examined whether the position of the NanoTags affects recognition by
32 the nanobodies. We generated H2B-mCherry, mito-mCherry, and CD8-mCherry with
33 N-terminal, internal, or C-terminal NanoTags. When these vectors were co-
34 transfected with NbVHH05-GFP or Nb127D01-GFP in S2R+ cells, GFP and mCherry
35 co-localized with the expected cellular compartments (**Figure 1E-J**). Taken together,
36 our data show that both NbVHH05 and Nb127D01 can be used as CBs to visualize
37 and monitor NanoTagged proteins in their native surroundings.

38 39 **Detecting NanoTagged proteins by immunofluorescence**

40 In addition to establishing CB-based detection of NanoTagged proteins in cells, we
41 also explored detection by immunofluorescence. Nanobodies can be detected by
42 either direct or indirect immunofluorescence. Direct immunofluorescence involves the
43 use of fluorophore-conjugated nanobodies to detect the target protein(s). Indirect

1 immunofluorescence involves recognition of the target by the nanobody, followed by
2 detection of the nanobody by a secondary fluorophore-conjugated antibody.

3 For direct immunofluorescence, we chemically conjugated NbVHH05 and
4 Nb127D01 with fluorophores (NbVHH05-555 and Nb127D01-647). Success of these
5 conjugations was confirmed by detection of a fluorescent signal on an SDS-PAGE
6 gel (**Figure 2—figure supplement 1**). Immunostaining with these fluorophore-
7 conjugated nanobodies directly revealed VHH05- and 127D01-tagged proteins in
8 S2R+ cells (**Figure 2A,A'**; **Figure 2—figure supplement 2A1,A2**). Direct
9 immunostaining with fluorophore-conjugated nanobodies thus provides a simple and
10 efficient method of detection. The reactivity of neither VHH05 nor 127D01 was
11 affected by direct chemical conjugation. In addition, we used a fluorescent
12 NbVHH05-555 prepared by sortase labeling (*Guimaraes et al., 2013*) (**Figure 2—**
13 **figure supplement 2A3**). These chemoenzymatic reactions proceed near-
14 quantitatively and are absolutely site-specific. Unlike chemical modification, the
15 sortase labeling procedure does not entail the risk of unwanted side reactions that
16 might otherwise affect the physicochemical properties of the final product. Because
17 each enzymatically modified nanobody carries a single substituent (fluorophore or
18 biotin), quantitative comparisons are in principle possible, which would be more
19 challenging when using direct chemical conjugation.

20 To test VHH05 and 127D01 in indirect immunofluorescence, we prepared
21 bacterially purified NbVHH05 and Nb127D01, each fused with an ALFA-tag or HA-
22 tag. We also prepared conditioned media that contained NbVHH05 or Nb127D01
23 tagged with the Fc portion of human IgG (hIgG) (**Figure 2—figure supplement**
24 **2B1**). Likewise, we could visualize NbVHH05-hIgG and Nb127D01-hIgG using
25 fluorescently labeled anti-human IgG antibodies (**Figure 2—figure supplement**
26 **2B1**). Consistent with a previous report (*Götzke et al., 2019*), NbVHH05-ALFA and
27 Nb127D01-ALFA can be visualized using anti-ALFA nanobodies conjugated to
28 fluorophores (**Figure 2; Figure 2—figure supplement 2B2**). We could visualize
29 NbVHH05-HA and Nb127D01-HA using fluorescently labeled anti-HA antibodies
30 (**Figure 2—figure supplement 2B3**). Next, we determined whether ALFA-, HA-, or
31 hIgG-tagged NbVHH05 and Nb127D01 could be used as the primary reagents for
32 indirect immunostaining. We stained S2R+ cells transfected with mito-GFP-VHH05 or
33 mito-GFP-127D01 vectors with the corresponding primary and secondary antibodies.
34 In both cases, the GFP signal overlapped completely with the fluorescent signal from
35 the secondary antibody (**Figure 2B'**; **Figure 2—figure supplement 2B**). NbVHH05
36 and Nb127D01 were obtained by immunization of an alpaca and llama, respectively
37 (*Ling et al., 2019; Bradley et al., 2015*). We therefore examined whether they are
38 both recognized by fluorophore-conjugated anti-alpaca IgG 647 which is reactive with
39 llama-derived nanobodies (or the VHH domain of llama IgG) (**Figure 2C**). The
40 NanoTagged GFP and 647-fluorophore signals overlapped completely (**Figure 2C'**;
41 **Figure 2—figure supplement 2B4**), indicating that commercially available
42 secondary antibodies against llama are compatible with NbVHH05 and Nb127D01
43 immunostaining. In addition, we carried out indirect immunofluorescence using
44 NbVHH05-biotin prepared by sortase labeling (*Guimaraes et al., 2013*) and obtained

1 similar results (**Figure 2—figure supplement 2B5**).

2 The availability of two different NanoTag-nanobody pairs opens the possibility for
3 co-staining or co-detection with CBs. To test this, we generated proteins tagged with
4 both NanoTags (VHH05- and 127D01-tags) and used NbVHH05 and Nb127D01
5 fused to HA-tag or ALFA-tag with corresponding secondary antibodies for detection.
6 Importantly, these two tagging systems operate orthogonally, as no co-localization
7 signal was observed in cells transfected with 127D01-GFP and with H2B-mCherry-
8 VHH05 or mito-mCherry-VHH05 (VHH05-GFP with H2B-mCherry-127D01 or mito-
9 mCherry-127D01) (**Figure 2—figure supplement 3A**). To further test co-detection,
10 we inserted VHH05 at the N-terminus of the transcription factor REPTOR and
11 127D01 at its C-terminus (VHH05-REPTOR-127D01). When S2R+ cells were
12 transfected with VHH05-REPTOR-127D01, the NbVHH05-HA signal (488-
13 fluorophore) and the Nb127D01-ALFA signal (647-fluorophore) completely
14 overlapped (**Figure 2D,D'**). Our data show that immunostaining using both of the
15 NanoTag-nanobody pairs can be multiplexed.

16 17 **Detection of NanoTagged proteins on immunoblots**

18 Because the two nanobodies recognize small linear epitopes, we anticipated that
19 these nanobodies might be useful for immunoblotting under denaturing conditions as
20 already shown for VHH05 (*Ling et al., 2015*). We performed immunoblotting
21 experiments with cell lysates containing VHH05- or 127D01-tagged H2B-mCherry.
22 Using NbVHH05-ALFA and Nb127D01-ALFA as primary nanobodies, we detected a
23 signal using NbALFA-HRP as the secondary antibody. Using purified nanobodies at
24 high concentrations (0.2 mg/ml) produced some non-specific bands. This issue was
25 resolved by reducing the nanobody concentration to 0.2 μ g/ml (**Figure 3—figure**
26 **supplement 1**). Next, we tested whether the two nanobodies could detect by
27 immunoblotting proteins NanoTagged in different positions. NbVHH05 and
28 Nb127D01 recognized proteins with internal, N- and C-terminal NanoTags on
29 immunoblots (**Figure 3A**). To test whether increasing the number of NanoTags
30 improved the sensitivity of detection, we generated vectors that express secreted
31 GFP with 1x, 2x or 3x-VHH05 or 127D01 Nanotags at the C-terminus (**Figure 3B**).
32 An N-terminal FLAG-tag was included in all constructs and used as the loading
33 control. An increase in the number of NanoTags improved the sensitivity of detection
34 using culture media that contain secreted GFP proteins (**Figure 3B**). Tagging of
35 target proteins with more than one copy of a tag thus improves the sensitivity of
36 detection.

37 Next, we tested whether the nanobodies against the VHH05 and 127D01 tags
38 could be used for multiplexed immunoblots by double-tagging the Upd2 cytokine
39 (VHH05-Upd2-127D01). As we needed to detect each nanobody in a specific
40 manner, we tagged one nanobody with the ALFA tag and detected it using NbALFA
41 and the other, with a human IgG (hIgG). We expressed and purified nanobody-hIgG
42 from S2 cells and tested different concentrations of conditioned media on
43 immunoblots (**Figure 3—figure supplement 2**). Very dilute conditioned media still
44 produced a strong signal, even though the nanobody-hIgG was not purified or

1 concentrated. After establishing working concentrations of hlgG-tagged nanobody
2 conditioned media, we performed multiplexed immunostaining using Nb127D01-hlgG
3 and NbVHH05-ALFA, or NbVHH05-hlgG and Nb127D01-ALFA, detected with anti-
4 human IgG and NbALFA, respectively (**Figure 3C**). Upd2 undergoes fragmentation
5 due to internal furin cleavage sites, which produced different bands on the
6 immunoblot. A combination of human IgG-tagged nanobody and ALFA-tagged
7 nanobody can thus be used for multiplexed immunoblotting (**Figure 3C**). In addition,
8 we confirmed that a combination of NbVHH05-biotin and Nb127D01-hlgG also
9 worked well for multiplexed immunoblotting (**Figure 3C**).

10 Another key application of antibodies is immunopurification of target proteins. To
11 explore whether NbVHH05 and Nb127D01 can be used for immunopurification, we
12 coated NbALFA resin with ALFA-tagged VHH05 or 127D01 nanobodies and used the
13 modified resin to recover NanoTagged FLAG-GFP secreted in S2 cell culture media.
14 FLAG-GFP-3xVHH05 and FLAG-GFP-3x127D01 were captured by NbVHH05-ALFA
15 and Nb127D01-ALFA, respectively (**Figure 3D,E**). Protein A magnetic beads coated
16 with Nb127D01-hlgG also successfully recovered FLAG-GFP-3x127D01 from S2 cell
17 culture media (**Figure 3F**). We confirmed that the VHH05 and 127D01 systems do
18 not cross-react (**Figure 2—figure supplement 3B**). NanoTag-based
19 immunopurification with these nanobodies is thus effective.

21 **NanoTag trap as a method to alter protein localization**

22 One of the many possible applications of nanobodies is to express them in cells or *in*
23 *vivo* as fusion proteins localized to a particular subcellular location, in order to
24 manipulate the localization of a NanoTagged POI. To test whether the
25 NbVHH05/VHH05-tag and Nb127D01/127D01-tag can be used to alter localization,
26 we constructed secreted GFP expression vectors that each had a N-terminal BiP
27 signal peptide and a C-terminal VHH05- or 127D01-tag (BiP-GFP-VHH05 and BiP-
28 GFP-127D01) (**Figure 4A,B**). We also constructed NbVHH05 and Nb127D01 with
29 mCherry and KDEL endoplasmic reticulum (ER) retention signal (BiP-Nanobody-
30 mCherry-KDEL), which should result in retention of the fusion protein in the ER
31 (**Figure 4A,B**). When transfecting only BiP-GFP-VHH05 or BiP-GFP-127D01 into
32 S2R+ cells, we did not observe GFP accumulation within cells, as the GFP fusion
33 was actively secreted into the culture medium (**Figure 4C**). However, after co-
34 transfecting BiP-NbVHH05-mCherry-KDEL with BiP-GFP-VHH05, or BiP-Nb127D01-
35 mCherry-KDEL with BiP-GFP-127D01, we observed intracellular accumulation of
36 GFP that colocalized with the mCherry signal. This shows that NanoTagged-GFP
37 proteins directed to the secretory pathway can be trapped by an ER NanoTag trap
38 (i.e. nanobodies with an ER retention signal) (**Figure 4C**). Indeed, cell lysates
39 prepared from cells transfected with ER NanoTag trap showed more GFP signal on
40 immunoblot, compared to controls lacking the ER NanoTag trap (**Figure 4D**).

41 We also prepared membrane-tethered nanobodies (membrane NanoTag trap) in
42 order to re-localize cytoplasmic NanoTagged proteins to the membrane (**Figure 4—**
43 **figure supplement 1A,B**). When S2R+ cells were co-transfected with CD8-
44 NbVHH05-GFP/mito-mCherry-VHH05 or CD8-Nb127D01-GFP/mito-mCherry-

1 127D01, mCherry colocalized with GFP on the cell membrane (**Figure 4—figure**
2 **supplement 1C**). NanoTag traps targeted to particular cellular compartments can
3 thus alter the subcellular distribution of NanoTagged proteins. The ability to do so
4 may facilitate a variety of functional analyses.

5

6 **Assessing NanoTags *in vivo***

7 The successful use of the NbVHH05/VHH05-tag and Nb127D01/127D01-tag in cells
8 prompted us to test them *in vivo*. We first constructed a series of UAS vectors with
9 either a cytoplasmic or secreted version of the two nanobodies, tagged with GFP or
10 HA (**Figure 5—figure supplement 1A**), and tested them in cells. As expected, when
11 transfected together with the *pAct-Gal4* plasmid, the cytoplasmic expression vectors
12 led to an expression of nanobodies detectable in S2R+ cell lysates, and the secretory
13 expression vectors resulted in detection of nanobodies predominantly in the culture
14 media (**Figure 5—figure supplement 1B,C**). Next, we generated transgenic flies
15 carrying these UAS constructs. We did not expect NbVHH05 or Nb127D01 to interact
16 with any fly endogenous proteins for lack of obvious sequence similarity between the
17 *Drosophila* proteome and the amino acid sequence of the two tags (data not shown).
18 To confirm this experimentally, we ubiquitously expressed NbVHH05 or Nb127D01 *in*
19 *vivo* throughout development using *tubulin-Gal4*. The nanobodies were not toxic to
20 flies; we readily obtained adult *tubulin-Gal4*, *UAS-Nanobody* flies and did not observe
21 any detectable developmental defects or abnormalities (data not shown). To further
22 test these constructs, we used fat body-specific *Lpp-Gal4* to drive NbVHH05 or
23 Nb127D01 expression. Immunofluorescence showed that GFP- or HA-tagged
24 NbVHH05 or Nb127D01 is expressed at readily detectable levels in fat body cells
25 (**Figure 5A-D**). We also confirmed that nanobodies with the BiP signal peptide are
26 secreted (**Figure 5E,F**).

27 To address whether NanoTagged POIs can be detected *in vivo*, we generated
28 *UAS-VHH05-REPTOR-127D01* flies. A previous study has shown that in S2 cells, the
29 transcription factor REPTOR is enriched in the cytoplasm under normal conditions
30 but translocates into the nucleus upon rapamycin treatment (*Tiebe et al., 2015*). To
31 test whether the changes in REPTOR localization can be detected using the
32 nanobodies, we co-expressed NanoTagged REPTOR along with Nb127D01-GFP or
33 NbVHH05-GFP specifically in adult enterocytes (ECs). In the absence of a
34 NanoTagged POI, Nb127D01-GFP and NbVHH05-GFP were detected in both the
35 cytoplasm and nuclei (**Figure 5G,I**). In contrast, when co-expressed with
36 NanoTagged REPTOR, the nanobody-GFP signals were enriched in the cytoplasm
37 of ECs under normal food conditions (**Figure 5H,J**). Following rapamycin treatment,
38 a stronger GFP signal was observed in nuclei. Similar changes were absent from
39 ECs that express Nb127D01-GFP or NbVHH05-GFP alone (**Figure 5G,I**). These
40 results confirm that rapamycin treatment leads to translocation of REPTOR into the
41 nucleus *in vivo* and provide further support for the idea that co-expression of
42 NanoTag POIs and nanobodies can visualize the subcellular location of a POI
43 (**Figure 5H,J**).

1 Next, we checked whether NanoTagged proteins can be detected *in vivo* using
2 purified nanobodies. We first constructed several vectors that contain NanoTags at
3 the N- or C-terminus of POIs and tested them in S2R+ cells. For secreted proteins,
4 we replaced the endogenous signal peptide with the BiP signal peptide (**Figure 5—**
5 **figure supplement 1D**). NanoTagged Akh, Dilp2, Dilp8, Pvf1, and Upd2 were readily
6 detected in the culture media using NbVHH05 or Nb127D01 (**Figure 5—figure**
7 **supplement 1E**). REPTOR and two isoforms of REPTOR-BP (REPTOR-BP-B and
8 REPTOR-BP-C) could also be detected using NbVHH05 or Nb127D01 from
9 transfected S2R+ cell lysates (**Figure 5—figure supplement 1F,G**). In addition to
10 *VHH05-REPTOR-127D01* flies, we also generated a version of Upd2 with the BiP
11 secretion signal and both NanoTags for *in vivo* study. We used *Myo1A^{ts}* to drive
12 *UAS-BiP-VHH05-Upd2-127D01* and were able to detect the signal in adult midguts,
13 using either NbVHH05 or Nb127D01 for detection by immunofluorescence (**Figure**
14 **5—figure supplement 2**). Taken together, these data indicate that both
15 NbVHH05/VHH05 and Nb127D01/127D01 work well for *in vivo* imaging and
16 immunostaining.

17

18 **CRISPR-mediated tagging of endogenous genes with NanoTags**

19 In many cases, tagging endogenous proteins is preferable to UAS-based
20 overexpression of tagged cDNAs, as UAS/Gal4-mediated expression can exceed
21 physiological levels. Further, while many proteins have been tagged endogenously
22 with GFP (*Morin et al., 2001; Sarov et al., 2016; Li-Kroeger et al., 2018*), tagging with
23 smaller epitope tags may be preferable to minimize their structural impact. To tag
24 endogenous genes with either VHH05-tag or 127D01-tag, we used a standard
25 CRISPR-Cas9 targeted insertion method to tag fly proteins at their N- or C- terminus
26 via the homology directed repair (HDR) pathway (**Figure 6—figure supplement**
27 **1A,B,C**). To facilitate this approach, we first designed four universal vectors based
28 on the scarless editing CRISPR knock-in approach (*Lamb et al., 2017*). Each vector
29 contains four common features: *3xP3-dsRed-SV40* for identification of transformants,
30 5'/3' terminal repeats for piggyBac transposase recognition sequences, TTA for
31 piggyBac target sequence, and an EcoRI restriction site for cloning target locus
32 homologous arms by Gibson assembly (**Figure 6—figure supplement 1A'**). We
33 chose Histone H2A variant (H2Av) as an example, because the expected nuclear
34 localization of H2Av should be easily visualized. We cloned the sequence 1 kb
35 upstream and 1 kb downstream of the stop codon (TAA) into the donor vector
36 (**Figure 6—figure supplement 2A**). An sgRNA plasmid that targeted a seed
37 sequence near the TAA of H2Av gene was injected into *yw; nos-cas9/CyO* embryos
38 together with the donor plasmid (**Figure 6—figure supplement 1B'**). Positive
39 transformants with red fluorescent eyes were outcrossed and successful knock-in
40 events were confirmed by junction PCR and sequencing (**Figure 6—figure**
41 **supplement 1C'**). Subsequently, 3xP3dsRed was excised using piggyBac
42 transposase (**Figure 6—figure supplement 2B**). After sequence verification (**Figure**
43 **6—figure supplement 2C**), we immunostained midguts from H2Av-3x127D01- and
44 H2Av-3xVHH05-expressing flies using Nb127D01-HA/NbVHH05-HA or NbVHH05-

1 555/NbVHH05-biotin. As shown in **Figure 6—figure supplement 1D'** and **Figure**
2 **6—figure supplement 2D**, H2Av tagged with either NanoTag was clearly observed
3 in the nucleus, demonstrating that this tagging method can be used effectively to
4 engineer NanoTagged forms of POIs and study their localization and/or function at
5 physiological expression levels.

6 In order to further test the sensitivity and the possibility of labeling secreted
7 small peptides by the KI method, we selected *Dilp2* as an example. The above
8 results showed that the double NanoTagged Dilp2 can be secreted into S2R+ culture
9 medium and detected by western blot using NbVHH05 or Nb127D01 (**Figure 5—**
10 **figure supplement 1F**). Here, we integrated 3x127D01 into the C-terminal of
11 endogenous *Dilp2* using KI strategy (**Figure 6A,B,C**). After confirming the proper
12 integration (**Figure 6D**), we compared Nb127D01 and Dilp2 antibody stainings in the
13 larval brain, which revealed similar expression patterns (**Figure 6E**; *Park et al.*,
14 2014). Since introducing tags to proteins can negatively affects their functions and a
15 previous study has shown that *Dilp2* RNAi increases trehalose levels (*Broughton et*
16 *al.*, 2008), we examined the trehalose level of 127D01-tagged Dilp2 expressing flies.
17 No difference was observed compared to control (**Figure 6G**), suggesting that that
18 NanoTagged Dilp2 is functional. Furthermore, the change in Dilp2 signal in IPC cells
19 and their neuronal projections in larval brain after starvation was easily detected by
20 Nb127D01 immunostaining (**Figure 6G**). These results indicate that the CRISPR-
21 mediated tagging of endogenous genes with NanoTags can be used for detecting
22 small peptides with high sensitivity.

23 24 **Discussion**

25 In this study, we characterized two NanoTags, VHH05 and 127D01, and their
26 corresponding nanobodies, for use in *Drosophila* for cellular and *in vivo* studies. We
27 show that these two systems can be used for *in vivo* detection via CBs, re-
28 localization, direct or indirect immunostaining, immunoblotting, and
29 immunopurification. The observation that these nanobodies recognize the NanoTags
30 on immunoblots is particularly useful, as only few nanobodies that recognize a
31 defined amino acid sequence have been characterized as suitable for
32 immunoblotting (*Cheloha et al.*, 2020) The utility of this system is further enhanced
33 by ease of purification of nanobodies from either bacterial cells or *Drosophila* cultured
34 cells. Modification of these nanobodies with ALFA or HA tags facilitates detection.
35 Installation of a human Fc portion on these nanobodies enables the use of anti-IgG
36 antibodies as secondary reagents for detection. In addition, we used chemical
37 labeling or site-specific sortase labeling to prepare nanobodies labeled with
38 fluorophores or biotin. We have thus developed reagents with broad applicability in
39 *Drosophila* research and beyond.

40 The system described here has significant advantages over conventional
41 antibodies or anti-GFP nanobodies. Nanobodies, unlike conventional antibodies, are
42 easily encoded as a single open reading frame in the genomes of model organisms
43 or cells. In addition, the small size of the NanoTags may be preferable in many cases
44 to GFP, as GFP is bulky and may affect the function of the tagged protein. Also, the

1 relatively long protein maturation time of GFP limit its use for imaging nascent
2 proteins. Finally, the anti-GFP nanobody, as used in deGradFP (*Caussinus et al.*,
3 2011), only poorly recognizes unfolded GFP.

4 We show how these short tags can be introduced into endogenous genes, using
5 the scarless CRISPR knock-in editing approach. Given the small size of the tags,
6 additional methods for genome modification deserve to be explored. For example,
7 ssDNA based CRISPR knock-in can be used to insert short sequences into a precise
8 location in the genome (*Ling et al.*, 2017). Another possibility is prime editing, which
9 relies on pegRNAs to insert sequences smaller than 48 bp into a chosen genomic
10 position (*Anzalone et al.*, 2019; *Bosch et al.*, 2021).

11 A key feature of the NanoTag/nanobody system is the ability to co-express the
12 nanobody *in vivo* in the form of a CB or some other fusion. We show that this
13 approach can be used to re-localize proteins. Expression *in vivo* also opens the
14 doors to using versions of the deGrad system or other functional fusions to
15 manipulate proteins in other ways (*Caussinus and Affolter*, 2016). Some S2R+ cells
16 transfected with Nb127D01-GFP contained aggregates (data not shown). However,
17 we did not observe aggregates in Nb127D01-mCherry transfected cells or transgenic
18 Nb127D01-GFP flies, nor did we observe developmental defects or effects on
19 viability following expression of the tags and/or nanobodies *in vivo*. The occasional
20 observation of protein aggregation in cells more likely reflects the high level of
21 expression when transfecting cells with exogenous expression constructs.

22 Given their versatility and *in vivo* applications, we anticipate that the two
23 NanoTags and corresponding nanobodies will be useful to address many cell
24 biological questions. The relative ease with which the system can be used for *in vivo*
25 tagging, as well as our demonstration that the system can be used in a number of
26 ways for imaging (i.e. using CBs or direct or indirect immunofluorescence) are
27 obvious assets. The NanoTag approach might be particularly useful for the new and
28 growing need to spatially map cell clusters identified from scRNAseq studies (*Mohr et*
29 *al.*, 2021). Other potential applications for *in vivo* tagged proteins include
30 chromosome immunoprecipitation (ChIP), immunopurification of protein complexes,
31 and inducing degradation of proteins that carry the tag (e.g. as shown for GFP in
32 *Caussinus et al.*, 2011; *Neumuller et al.*, 2012). Another benefit of double labeling is
33 that nanobody binding (for manipulation) may prohibit subsequent detection of the
34 protein by the same nanobody; for example, when membrane localized Nanobody 1
35 is used to manipulate the localization of Protein X-NanoTag 1, Nanobody 1 cannot be
36 used to visualize Protein X-NanoTag 1. This issue can be resolved with double
37 NanoTagged proteins (NanoTag2-proteinX-Nanotag1), as Nanobody 2-Fluorophore
38 should allow detection when membrane-localized Nanobody 1 is used as a trap.

39 Although we developed and validated the NanoTag system for use in
40 *Drosophila*, the same approaches should be applicable to other systems. The mouse
41 genome contains a predicted amino acid sequence with 100% identity to the epitope
42 recognized by VHH05, which is not surprising, given that the tag sequence is
43 identical to a segment of the human source protein, Ube6e. For 127D01, however,
44 no proteins encoded by the mouse genome have peptides with more than 50%

1 identity to the tag, suggesting that 127D01 could be used for murine studies.
2 Moreover, there are no peptides with more than 50% identity to either tag in many
3 species of research interest, including *E. coli*, *Saccharomyces cerevisiae*, *C.*
4 *elegans*, *Arabidopsis thaliana*, *Oryza sativa* (rice), the mosquitoes *Aedes aegypti*,
5 *Anopheles gambiae* and *Anopheles stephensi*, *Bombyx mori* (silkworm), *Tribolium*
6 *castaneum* (red flour beetle), *Danaus plexippus* (monarch butterfly), and *Danio rerio*
7 (zebrafish), suggesting that both tags could be used in these organisms.
8

9 **Materials and methods**

10 **Key resources table**

REAGENT or RESOURCE	SOURCE	IDENTIFIER
Antibodies, nanobodies		
Mouse anti- α -Tubulin	Sigma-Aldrich	Cat# T5168; RRID: AB_477579
Mouse anti-GFP	Invitrogen	Cat# A11120; RRID: AB_221568
Rat anti-HA	Sigma-Aldrich	Cat# 3F10; RRID: AB_2314622
Mouse anti-FLAG M1	Sigma-Aldrich	Cat# F3040; RRID: AB_439712
Rabbit anti-Dilp2	Park et al., 2014	N/A
NbALFA-HRP	NanoTag Biotechnologies	Cat# N1502-HRP
NbALFA-Atto647	NanoTag Biotechnologies	Cat# N1502-At647N-L
NbALFA-800CW	NanoTag Biotechnologies	Cat# N1502-Li800-L
Goat Anti-Alpaca IgG-647	Jackson ImmunoResearch	Cat# 128-605-230
Mouse anti-HA-Alexa Fluor 488	Thermo Fisher Scientific	Cat# A-21287
Goat Anti-Human IgG Fc-HRP	Thermo Fisher Scientific	Cat# A18829
Donkey anti-Human IgG-DyLight 680	Thermo Fisher Scientific	Cat# SA5-10130
Streptavidin-DyLight 800	Thermo Fisher Scientific	Cat# 21851
Streptavidin-Alexa Fluor 488	Thermo Fisher Scientific	Cat# S32354
NbVHH05-HA	This paper	N/A
NbVHH05-ALFA	This paper	N/A
NbVHH05-hIgG	This paper	N/A
NbVHH05-555	This paper	N/A
NbVHH05-biotin (sortagging)	This paper	N/A
NbVHH05 -555 (sortagging)	This paper	N/A
Nb127D01-HA	This paper	N/A
Nb127D01-ALFA	This paper	N/A
Nb127D01-hIgG	This paper	N/A
Nb127D01-647	This paper	N/A

Chemicals, Peptides, and
Recombinant Proteins

Phusion polymerase	New England Biolabs	Cat# M0530
Q5 polymerase	New England Biolabs	Cat# M0494
Taq polymerase	Clontech	Cat# TAKR001
EcoRI	New England Biolabs	Cat# R0101
XbaI	New England Biolabs	Cat# R0145
BglII	New England Biolabs	Cat# R0144
NheI	New England Biolabs	Cat# R3131
NsiI-HF	New England Biolabs	Cat# R3127
NcoI-HF	New England Biolabs	Cat# R3193
XhoI	New England Biolabs	Cat# R0146
BbsI	New England Biolabs	Cat# R0539
AarI	Thermo Fisher Scientific	Cat# ER1581
T4PNK	New England Biolabs	Cat# M0201
T4 DNA ligase	New England Biolabs	Cat# M0202
fetal bovine serum	Sigma-Aldrich	Cat# A3912
Schneider's media	Thermo Fisher Scientific	Cat# 21720-024
penicillin-streptomycin	Thermo Fisher Scientific	Cat# 15070-063
ESF921 media	Expression Systems	Cat# 96-001
proteinase K	Roche	Cat# 3115879001
RNase A	Thermo Fisher Scientific	Cat# EN0531
protease and phosphatase inhibitor cocktail	Pierce	Cat# 78440
trypsin inhibitor benzamidine	Sigma-Aldrich	Cat# 434760
4',6-diamidino-2-phenylindole (DAPI)	Thermo Fisher Scientific	Cat# D1306
rapamycin	LC Laboratories	Cat# R-5000
HRP-Conjugated Streptavidin	Thermo Fisher Scientific	Cat# N100
Trehalase (prokaryote)	Megazyme	Cat# E-TREH

Critical Commercial Assays

Gibson assembly	New England Biolabs	Cat# E2611
NEBuilder HiFi assembly	New England Biolabs	Cat# E2621
Golden Gate Assembly	New England Biolabs	Cat# E1601
pJET-1.2 vector kit	Fermentas	Cat# K1231
QIAquick Gel Extraction Kit	Qiagen	Cat# 28706
QIAquick Spin Columns	Qiagen	Cat# 28115
Effectene	Qiagen	Cat# 301427
B-PER II Bacterial Protein Extraction Reagent	Thermo Fisher Scientific	Cat# 78260

Mix-n-Stain CF 555 Antibody Labeling Kit	Sigma-Aldrich	Cat# MX555S100
Mix-n-Stain CF 647 Antibody Labeling Kit	Sigma-Aldrich	Cat# MX647S100
Ni-NTA resin	EMD Millipore	Cat# 70691-3
PD-10 column	GE Healthcare	Cat# GE17-0851-01
lysis buffer	Pierce	Cat# 87788
SDS sample buffer	Thermo Fisher Scientific	Cat# 39001
4%-20% polyacrylamide gel	Bio-Rad	Cat# 4561096
enhanced chemiluminescence (ECL) reagents	Amersham	Cat# RPN2209
enhanced chemiluminescence (ECL) reagents	Pierce	Cat# 34095
ALFA Selector ST resin	Nanotag Biotechnologies	Cat# N1511
Pierce IP lysis buffer	Thermo Fisher Scientific	Cat# 87787
Protein A Magnetic Beads	Bio-Rad	Cat# 1614013
tetramethylbenzidine-containing solution	Thermo Fisher Scientific	Cat# N301
Glucose Hexokinase Reagents	Thermo Fisher Scientific	Cat# TR15421
Plasmids		
pAW	Perrimon lab	N/A
pWalium10	DGRC	Cat# 1470
pMK-33GW	Perrimon lab	N/A
pET-26b	Novagen	Cat# 69862
pQUASp-mCD8mCherry	Addgene	Cat# 46164
pBac (3xP3-gTc ^v ; pUb:lox-mYFP-lox-H2BmCherry)	Addgene	Cat# 119064
pcDNA4TO-mito-mCherry-10xGCN4_v4	Addgene	Cat# 60914
PXL-IE1-EGFP-nos-Cas9	Xu et al., 2020	N/A
pScarlessHD-2xHA-DsRed	Addgene	Cat# 80822
pCFD3	Addgene	Cat# 49410
pAW-NbVHH05-GFP	This paper	N/A
pAW-Nb127D01-GFP	This paper	N/A
pAW-NbVHH05-mCherry	This paper	N/A
pAW-Nb127D01-mCherry	This paper	N/A
pAW-H2B-mCherry-VHH05	This paper	N/A
pAW-mito-mCherry-VHH05	This paper	N/A
pAW-CD8-mCherry-VHH05	This paper	N/A
pAW-H2B-mCherry-127D01	This paper	N/A

pAW-mito-mCherry-127D01	This paper	N/A
pAW-CD8-mCherry-127D01	This paper	N/A
pAW-VHH05-H2B-mCherry	This paper	N/A
pAW-CD8-VHH05-mCherry	This paper	N/A
pAW-127D01-H2B-mCherry	This paper	N/A
pAW-CD8-127D01-mCherry	This paper	N/A
pAW-BiP-NbVHH05-mCherry-KDEL	This paper	N/A
pAW-BiP-Nb127D01-mCherry-KDEL	This paper	N/A
pAW-CD8-NbVHH05-GFP	This paper	N/A
pAW-CD8-Nb127D01-GFP	This paper	N/A
pAW-HGP-BiP-FLAG-GFP-VHH05	This paper	N/A
pAW-HGP-BiP-FLAG-GFP-2xVHH05	This paper	N/A
pAW-HGP-BiP-FLAG-GFP-3xVHH05	This paper	N/A
pAW-HGP-BiP-FLAG-GFP-127D01	This paper	N/A
pAW-HGP-BiP-FLAG-GFP-2x127D01	This paper	N/A
pAW-HGP-BiP-FLAG-GFP-3x127D01	This paper	N/A
pW10-UAS-BiP-127D01-Akh-VHH05	This paper	N/A
pW10-UAS-BiP-127D01-Dilp2-VHH05	This paper	N/A
pW10-UAS-BiP-127D01-Dilp8-VHH05	This paper	N/A
pW10-UAS-BiP-127D01-Pvf1-VHH05	This paper	N/A
pW10-UAS-127D01-REPTOR-bp-B-VHH05	This paper	N/A
pW10-UAS-127D01-REPTOR-bp-C-VHH05	This paper	N/A
pMT-HGP-v3-Nb127D01-hlgG	This paper	N/A
pMT-HGP-v3-NbVHH05-hlgG	This paper	N/A
pET-26b-Nb127D01-HA-His	This paper	N/A
pET-26b-NbVHH05-HA-His	This paper	N/A
pET-26b-Nb127D01-ALFA-His	This paper	N/A
pET-26b-NbVHH05-ALFA-His	This paper	N/A
pW10-UAS-NbVHH05-HA	This paper	N/A
pW10-UAS-BiP-NbVHH05-HA	This paper	N/A
pW10-UAS-Nb127D01-HA	This paper	N/A
pW10-UAS-BiP-Nb127D01-HA	This paper	N/A
pW10-UAS-NbVHH05-GFP	This paper	N/A
pW10-UAS-BiP-NbVHH05-GFP	This paper	N/A
pW10-UAS-Nb127D01-GFP	This paper	N/A
pW10-UAS-BiP-Nb127D01-GFP	This paper	N/A
pW10-UAS-127D01-REPTOR-VHH05	This paper	N/A

pW10-UAS-BiP-127D01-Upd2-VHH05	This paper	N/A
pW10-UAS-BiP-127D01-Akh-VHH05	This paper	N/A
pCFD3-H2Av-sgRNA	This paper	N/A
pScarlessHD-C-3x127D01-H2Av-DsRed	This paper	N/A
pScarlessHD-C-3xVHH05-H2Av-DsRed	This paper	N/A
pScarlessHD-C-3x127D01-DsRed	This paper	N/A
pScarlessHD-C-3xVHH05-DsRed	This paper	N/A
pScarlessHD-N-3x127D01-DsRed	This paper	N/A
pScarlessHD-N-3xVHH05-DsRed	This paper	N/A

Experimental Models: Cell Lines

S2R+	DGRC	Cat# 150
ESF921-adapted S2 cells	This paper	N/A

Experimental Models:

Organisms/Strains

w1118	Perrimon lab	N/A
y,v; P{nos- phiC31\int.NLS}X; P{CaryP}attP40	Perrimon lab	N/A
y,w; P{nos- phiC31\int.NLS}X; P{CaryP}attP2	Perrimon lab	N/A
y,w; nos-Cas9/CyO	Perrimon lab	N/A
y,w; TM3, Sb/TM6, Tb	Perrimon lab	N/A
yw; Gla/CyO	Perrimon lab	N/A
yw; If/CyO; MKRS/TM6, Tb	Perrimon lab	N/A
Myo1A-Gal4, tub-Gal80 ^{ts}	Perrimon lab	N/A
Lpp-Gal4	Perrimon lab	N/A
yw; UAS-NbVHH05-HA, w+ attp2	This paper	N/A
yw; UAS-NbVHH05-HA, w+ attp40	This paper	N/A
yw; UAS-Nb127D01-HA, w+ attp2	This paper	N/A
yw; UAS-Nb127D01-HA, w+ attp40	This paper	N/A
yw; UAS-NbVHH05-GFP, w+ attp2	This paper	N/A
yw; UAS-NbVHH05-GFP, w+ attp40	This paper	N/A
yw; UAS-Nb127D01-GFP, w+ attp2	This paper	N/A
yw; UAS-Nb127D01-GFP, w+ attp40	This paper	N/A
yw; UAS-BiP-NbVHH05-HA, w+ attp2	This paper	N/A
yw; UAS-BiP-NbVHH05-HA, w+ attp40	This paper	N/A

yw; UAS-BiP-Nb127D01-HA, w+ attp2	This paper	N/A
yw; UAS-BiP-Nb127D01-HA, w+ attp40	This paper	N/A
yw; UAS-BiP-NbVHH05-GFP, w+ attp2	This paper	N/A
yw; UAS-BiP-NbVHH05-GFP, w+ attp40	This paper	N/A
yw; UAS-BiP-Nb127D01-GFP, w+ attp2	This paper	N/A
yw; UAS-BiP-Nb127D01-GFP, w+ attp40	This paper	N/A
yw; UAS-BiP-VHH05-Upd2-127D01, w+ attp40	This paper	N/A
yw; UAS-VHH05-REPTOR-127D01, w+ attp40	This paper	N/A
w; H2Av-3xVHH05/TM3, Sb	This paper	N/A
w; H2Av-3x127D01/TM3, Sb	This paper	N/A
TOP10 <i>Escherichia coli</i>	Invitrogen	Cat# C404010
BL21 (DE3) <i>Escherichia coli</i>	New England Biolabs	Cat# C25271
Oligonucleotides		
All oligos	This paper	See Table S1
Software		
Photoshop	Adobe	N/A
ImageJ	NIH	N/A
Excel	Microsoft	N/A
GraphPad Prism6	GraphPad	N/A
Other		
Joystick Micromanipulator	NARISHIGE	Cat# MN-151
FemtoJet Microinjector	Eppendorf	Cat# LV41365120
Garfunkel Nikon Ti2 Spinning Disk	Nikon	N/A
Kimble Kontes pellet pestles	Millipore	Cat# Z359947
Immobilon-P polyvinylidene fluoride (PVDF) membrane	Millipore	Cat# IPVH00010
ChemiDoc MP imaging system	Bio-Rad	Cat# 17001402
Kodak M35 X-OMAT Automatic Processors	KODAK	Cat# RT-KP-M35A
Hyperfilm™ ECL™	Amersham	Cat# GE28-9068-35

1

2

Plasmids construction

1 Four types of vectors were used in this study: 1. pAW, that contains the fly actin5C
2 promoter; 2. pWalium10, a UAS/Gal4 vector that contains a UAS promoter and mini-
3 white selection marker (DGRC, 1470); 3. pMT (pMK-33GW, Ram Viswanatha); and
4 4. pET-26b (Novagen 69862). pAW-HGP-sortase is a pAW vector derivative with N-
5 terminal BiP signal peptide/FLAG-tag, AarI-cloning site for Gibson or HiFi assembly,
6 C-terminal purification tag with Sortase-tag and His-tag, and heat shock promoter-
7 GFP-T2A-PuroR for stable cell line generation. pMT-HGP-v3 is a pMT vector
8 derivative with N-terminal BiP signal peptide/FLAG-tag, AarI-cloning site for Gibson
9 or HiFi assembly, C-terminal purification tag with Avi-tag and His-tag, and heat shock
10 promoter-GFP-T2A-PuroR for stable cell line generation. pET-26b-Nb-GGA is a pET-
11 26b derivative with BsaI Golden Gate Assembly cloning site flanked by pelB signal
12 sequence and C-terminal ALFA- and His-tags.

13 Plasmid DNAs were constructed and amplified using standard protocols. Briefly,
14 plasmids were linearized by restriction enzymes as described by the commercial
15 vendor. PCR fragments were amplified using Phusion polymerase (New England
16 Biolabs (NEB), M0530) or Q5 polymerase (NEB, M0494). Linearized plasmids and
17 PCR fragments were gel purified using QIAquick columns (Qiagen, #28115) and
18 joined using either Gibson assembly (NEB, E2611) or NEBuilder HiFi assembly
19 (NEB, E2621). Reactions were transformed into chemically competent TOP10
20 *Escherichia coli* (Invitrogen, C404010), plated and selected on lysogeny broth (LB)-
21 agar plates with ampicillin (100 µg/mL) or kanamycin (50 µg/mL). Colony PCR was
22 performed using Takara Taq polymerase (Clontech, TAKR001C). Plasmid DNA was
23 isolated from cultured bacteria using QIAprep Spin Miniprep Kit (Qiagen, 27104).
24 Plasmid sequences were confirmed by Sanger sequencing performed at the Dana-
25 Farber/Harvard Cancer Center DNA Resource Core or Genewiz. Primers sequences
26 are listed in Table S1.

27 **pW10-Nanobody variants.** All UAS constructs were cloned into the pWalium10
28 (pW10) vector. For pW10-NbVHH05-HA, pW10-Nb127D01-HA, pW10-NbVHH05-
29 GFP, pW10-Nb127D01-GFP, pW10-BiP-NbVHH05-HA, pW10-BiP-Nb127D01-HA,
30 pW10-BiP-NbVHH05-GFP, and pW10-BiP-Nb127D01-GFP, pW10 was first
31 linearized with EcoRI (NEB, R0101) and XbaI (NEB, R0145). NbVHH05 or
32 Nb127D01 were cloned from pHEN6-VHH05 or pHEN6-127D01 (Ploegh lab). GFP
33 was amplified from PXL-IE1-EGFP-nos-Cas9 (Xu *et al.*, 2020). PCR fragments were
34 joined together with the digested pW10 backbone by Gibson assembly. HA and BiP
35 were incorporated by adding overhanging sequences to the primers. For pW10-BiP-
36 VHH05-Akh-127D01, pW10-BiP-VHH05-Dilp2-127D01, pW10-BiP-VHH05-Dilp8-
37 127D01, pW10-BiP-VHH05-Pvf1-127D01 and pW10-BiP-VHH05-Upd2-127D01,
38 pW10 was first digested with EcoRI and XbaI. A BiP-VHH05-127D01 fragment was
39 made by annealing two oligos and ligated into the linearized pW10 to generate the
40 intermediate vector, pW10-BiP-VHH05-BgIII-127D01. Next, PCR fragments of *Akh*,
41 *Dilp2*, *Dilp8*, *Pvf1*, and *Upd2* were amplified from fly cDNAs and inserted into pW10-
42 UAS-BiP-VHH05-127D01 linearized by BgIII (NEB, R0144) by Gibson assembly. For
43 pW10-127D01-REPTOR-bp-B-VHH05, pW10-127D01-REPTOR-bp-C-VHH05 and
44 pW10-127D01-REPTOR-VHH05, pW10-BiP-VHH05-127D01 was digested with

1 EcoRI and BglII to remove BiP-VHH05. VHH05 was introduced N-terminal of PCR
2 fragments of *REPTOR-bp-B*, *REPTOR-bp-C* and *REPTOR* through overhanging
3 primers. PCR fragments were inserted into pW10-127D01 (EcoRI and BglII digested)
4 by Gibson assembly.

5 ***pAW-Nanobody/NanoTagged fluorophore variants.*** For pAW-NbVHH05-GFP,
6 pAW-Nb127D01-GFP, pAW-NbVHH05-mCherry, pAW-Nb127D01-mCherry, pAW-
7 H2B-mCherry-VHH05, pAW-H2B-mCherry-127D01, pAW-mito-mCherry-VHH05,
8 pAW-mito-mCherry-127D01, pAW-CD8-mCherry-VHH05, pAW-CD8-mCherry-
9 127D01, pAW-VHH05-H2B-mCherry, pAW-127D01-H2B-mCherry, pAW-BiP-
10 NbVHH05-mCherry-KDEL, pAW-BiP-Nb127D01-mCherry-KDEL, pAW-CD8-
11 NbVHH05-GFP and pAW-CD8-Nb127D01-GFP, pAW was first linearized with NheI
12 (NEB, R3131) and XbaI. NbVHH05-GFP and Nb127D01-GFP were amplified from
13 pW10-NbVHH05-GFP and pW10-Nb127D01-GFP. *CD8*, *mCherry* and *CD8-mCherry*
14 were cloned from pQUASp-mCD8mCherry (Addgene, #46164). *H2B-mCherry* was
15 cloned from pBac (3xP3-gTc'v; pUb:lox-mYFP-lox-H2BmCherry) (Addgene,
16 #119064). *mito-mCherry* was cloned from pcDNA4TO-mito-mCherry-10xGCN4_v4
17 (Addgene, #60914). BiP-NbVHH05 or BiP-Nb127D01 fragments were cloned from
18 pW10-UAS-BiP-NbVHH05-GFP, pW10-UAS-BiP-Nb127D01-GFP. PCR fragments
19 were joined together with the digested pAW backbone by Gibson assembly. VHH05-,
20 127D01-tags, or KDEL sequences were incorporated in the N- or C-terminus by
21 adding overhanging sequences to the primers. For pAW-CD8-VHH05-mCherry and
22 pAW-CD8-127D01-mCherry, we first digested pAW-CD8-mCherry-VHH05 with NheI
23 to obtain a linearized pAW-CD8 backbone. mCherry was amplified from pQUASp-
24 mCD8mCherry. VHH05 or 127D01 was introduced into the N-terminal of PCR
25 fragments with overhanging primer sequences. The NanoTag-mCherry PCR
26 fragment was inserted into pAW-CD8 by Gibson assembly.

27 ***pAW-HGP-BiP-GFP with 1x/2x/3x NanoTags.*** For pAW-HGP-BiP-GFP-VHH05,
28 pAW-HGP-BiP-GFP-2xVHH05, pAW-HGP-BiP-GFP-3xVHH05, pAW-HGP-BiP-GFP-
29 127D01, pAW-BiP-HGP-GFP-2x127D01, pAW-HGP-BiP-GFP-3x127D01, pAW-
30 HGP-sortase was first linearized by AarI (Thermo Scientific ER1581). N-terminal
31 GFP was amplified by PCR. C-terminal GFP with 1x/2x/3x NanoTags were prepared
32 by gene synthesis (Twist Bioscience). PCR fragment and C-terminal GFP with
33 NanoTags were joined together with the linearized pAW-HGP-sortase by NEBuilder
34 HiFi assembly.

35 ***pMT-HGP-v3-Nb127D01-hlgG, pMT-HGP-v3-NbVHH05-hlgG.*** For cloning of
36 the inducible Nb127D01-hlgG and NbVHH05-hlgG expression vectors, the pMT-
37 HGP-v3 vector was linearized by both AarI and NsiI-HF (NEB, R3127). Human IgG
38 Fc region was amplified from pCER243 (a gift of Aaron Ring at Yale).
39 NbVHH05/Nb127D01 and hlgG PCR fragments were inserted into pMT-HGP-v3
40 (digested by AarI and NsiI-HF) by NEBuilder HiFi assembly.

41 ***pET-26b-Nb127D01-ALFA-His, pET-26b-NbVHH05-ALFA-His, pET-26b-***
42 ***Nb127D01-HA-His, pET-26b-NbVHH05-HA-His.*** For cloning pET-26b-Nb127D01-
43 ALFA-His and pET-26b-NbVHH05-ALFA-His, NbVHH05/Nb127D01 PCR fragments
44 were cloned into pET-26b-Nb-GGA by BsaI-Golden Gate Assembly (NEB, E1601).

1 To make pET-26b-Nb127D01-HA-His and pET-26b-NbVHH05-HA-His,
2 NbVHH05/Nb127D01 PCR fragments with HA tag were cloned into pET-26b (NcoI,
3 NEB, R3193 and XhoI, NEB, R0146 digested) by HiFi assembly.

4 ***pScarless NanoTag vectors: pScarlessHD-C-3x127D01-DsRed,***
5 ***pScarlessHD-C-3xVHH05-DsRed, pScarlessHD-N-3x127D01-DsRed,***
6 ***pScarlessHD-N-3xVHH05-DsRed.*** 3x127D01 or 3xVHH05 were cloned from pAW-
7 HGP-BiP-GFP-3x127D01 or pAW-HGP-BiP-GFP-3xVHH05. 3xP3-DsRed was
8 cloned from pScarlessHD-2xHA-DsRed (Addgene, 80822). Then, 3x127D01 or
9 3xVHH05 and 3xP3-DsRed PCR fragments were inserted into pScarlessHD-2xHA-
10 DsRed backbone (EcoRI digested) by Gibson assembly.

11 ***pScarlessHD-C-3x127D01-H2Av-DsRed, pScarlessHD-C-3xVHH05-H2Av-***
12 ***DsRed.*** pScarlessHD-C-3x127D01-DsRed and pScarlessHD-C-3xVHH05-DsRed
13 were digested with EcoRI to obtain the pScarlessHD backbone and 3xP3-DsRed
14 fragment. Upstream and downstream sequences of TAA at the C-terminus of the
15 *H2Av* gene were cloned from *yw; nos-Cas9/Cyo* flies. Then, 3xP3-DsRed, upstream
16 and downstream fragments were inserted into pScarlessHD backbone by Gibson
17 assembly.

18 ***pCFD3-H2Av-sgRNA.*** pCFD3 (Addgene, #49410) was digested with BbsI (NEB,
19 R0539). sgRNA oligos following phosphorylation were annealed by T4PNK (NEB,
20 M0201) and inserted into a digested pCFD3 backbone by T4 DNA ligase (NEB,
21 M0202).

22

23 **Cell transfection**

24 *Drosophila* S2R+ cells were cultured at 25°C in Schneider's media (Thermo Fisher
25 Scientific, 21720-024) with 10% fetal bovine serum (Sigma, A3912) and 50 U/mL
26 penicillin-streptomycin (Thermo Fisher Scientific, 15070-063). S2R+ cells were
27 transfected using Effectene (Qiagen, 301427) following the manufacturer's
28 instructions. A total of 200ng of plasmid DNA per well was transfected 24-well plates.
29 The culture medium was replaced 24 hours after transfection.

30 To produce secreted GFP proteins with 1x/2x/3x NanoTags and Nanobodies
31 with human IgG, ESF921-adapted S2 cells (Expression Systems, 94-005S) were
32 transfected using PEI transfection methods and cultured in protein-free ESF921
33 media (Expression Systems, 96-001). For 6-well plate transfection, 2.4µg of DNA
34 and 7.4µg of PEI were mixed in 300µl of ESF921 media for 15-30 min and added to
35 2.7ml of S2 cell culture (2E6 cells/ml, final cell density). Alternatively, 50ml
36 suspension cells cultured in 250ml flask were transfected using the same proportion.
37 On day 2 from transfection, protein expression was induced with 700µM CuSO₄ for 5
38 days. Cleared conditioned media were collected after centrifugation and directly used
39 for immunostaining, western blot, and immunoprecipitation.

40

41 **Fly Strains and Generating transgenic flies**

42 Fly husbandry and crosses were performed under standard conditions at 25°C.
43 Injections were carried in-house. Fly strains used to generate transgenic lines were
44 attP lines: attP40 (*y,v; P{nos- phiC31}int.NLS}X; P{CaryP}attP40*) and attP2 (*y,w;*

1 *P{nos-phiC31\int.NLS}X; P{CaryP}attP2*). Fly strains used to generate KI lines were
2 *y,w; nos-Cas9/CyO*. For balancing chromosomes, fly stocks *y,w; TM3, Sb/TM6,Tb*,
3 *yw; Gla/CyO, yw; If/CyO; MKRS/TM6,Tb* were used. All lines recovered were
4 homozygous viable. Fly stocks are from the Perrimon fly stock unless stated
5 otherwise. Other fly stocks used in this study were *Lpp-Gal4* (Hong-Wen Tang) and
6 *Myo1A-Gal4, tub-Gal80^{ts}* (Afroditi Petsakou).

7 Transgenic flies generated in this study are as follows:

8 *yw; UAS-NbVHH05-HA, w+ attp2*
9 *yw; UAS-NbVHH05-HA, w+ attp40*
10 *yw; UAS-Nb127D01-HA, w+ attp2*
11 *yw; UAS-Nb127D01-HA, w+ attp40*
12 *yw; UAS-NbVHH05-GFP, w+ attp2*
13 *yw; UAS-NbVHH05-GFP, w+ attp40*
14 *yw; UAS-Nb127D01-GFP, w+ attp2*
15 *yw; UAS-Nb127D01-GFP, w+ attp40*
16 *yw; UAS-BiP-NbVHH05-HA, w+ attp2*
17 *yw; UAS-BiP-NbVHH05-HA, w+ attp40*
18 *yw; UAS-BiP-Nb127D01-HA, w+ attp2*
19 *yw; UAS-BiP-Nb127D01-HA, w+ attp40*
20 *yw; UAS-BiP-NbVHH05-GFP, w+ attp2*
21 *yw; UAS-BiP-NbVHH05-GFP, w+ attp40*
22 *yw; UAS-BiP-Nb127D01-GFP, w+ attp2*
23 *yw; UAS-BiP-Nb127D01-GFP, w+ attp40*
24 *yw; UAS-BiP-VHH05-Upd2-127D01, w+ attp40*
25 *yw; UAS-VHH05-REPTOR-127D01, w+ attp40*
26 *w; H2Av-3xVHH05/TM3, Sb*
27 *w; H2Av-3x127D01/TM3, Sb*

28 Transgenic flies were generated by phiC31 integration of attB-containing
29 plasmids into either attP40 or attP2 landing sites. Briefly, plasmid DNA was purified
30 on QIAquick columns and eluted in injection buffer (100 μ M NaPO₄, 5 mM KCl) at a
31 concentration of 200-400 ng/ μ L. Plasmid DNA was injected into ~100 fertilized
32 embryos (*y,v nos-phiC31int; attP40* or *y,w nos-phiC31int; attP2*) through
33 microinjection handle (NARISHIGE, Japan) with pressure control (FemtoJet,
34 Eppendorf). The progeny was outcrossed to screen for transgenic founder progeny
35 and the UAS insertions were isolated by screening for white+ eye color.

36 To generate KI flies, donor and sgRNA plasmids were mixed together and were
37 injected into ~100 fertilized embryos (*y,w; nos-Cas9/CyO*). Transformed lines were
38 isolated using a DsRed marker. To remove the DsRed cassette, transformed lines
39 were crossed to a line expressing PBac transposase (BL #8285). Resulting lines
40 were sequenced to confirm the insertion of 3x127D01 or 3xVHH05 to the C-terminal
41 of the *H2Av* or *Dilp2* gene.

42

43 **Targeted integration analysis**

1 Genomic DNA was extracted from the DsRed2-positive G1 adult animals by standard
2 sodium dodecyl sulfate (SDS) lysis-phenol buffer after incubation with proteinase K
3 (Roche, 3115879001), followed by RNase A (Thermo Fisher Scientific, EN0531)
4 treatment and purification. The 5'- and 3'-end junction fragments at the integration
5 event were cloned separately and sequenced. PCR conditions included 2 min of
6 denaturation at 95 °C; 30 cycles of 1 min at 95 °C, 30 s at 55 °C and 1min at 72 °C;
7 followed by a final extension at 72 °C for 10 min by using Takara Taq polymerase
8 (Clontech, #TAKR001). To remove the DsRed cassette, the genomic DNA was
9 extracted by the same method and PCR conditions included 2 min of denaturation at
10 95 °C; 30 cycles of 1 min at 95 °C, 30 s at 55 °C and 30 s at 72 °C; followed by a
11 final extension at 72 °C for 10 min. PCR products were sub-cloned into the pJET-1.2
12 vector (Fermentas, #K1231) and sequenced. Primer sequences are listed in the
13 Table S1.

14

15 **Rapamycin treatment**

16 For rapamycin treatment, rapamycin (LC Laboratories, R-5000) was dissolved in
17 DMSO and mixed into the media when preparing food vials. The rapamycin dose
18 was 50uM.

19

20 **Nanobody purification**

21 Nanobody expression vectors with C-terminal ALFA-tag or HA-tag for bacterial
22 expression and purification were cloned into pET-26b-Nb-GGA or pET-26b by
23 Golden-Gate assembly or Gibson cloning, respectively. After transformation with
24 BL21 (DE3) competent cells (NEB, C25271), overnight cultures were inoculated in
25 LK media and incubated at 37°C until the OD600 approached ~0.6. Then, 0.1mM
26 IPTG was added and cultures were placed at 15°C for overnight. After centrifugation,
27 the cell pellet was collected and resuspended in B-PER II Bacterial Protein Extraction
28 Reagent (Thermo Scientific, 78260). After 30 min incubation with rotation, an
29 additional 19X volume of TBS was added and further incubated with rotation. Cleared
30 supernatants were collected after centrifugation at 20,000 g & 4°C for 15 min and
31 used for His-tag purification. Dialyzed His-tag purified nanobody fractions were
32 diluted at 0.2mg/ml concentration, which were directly used for immunostainings and
33 western blots. To generate fluorescent-labeled nanobodies, Mix-n-Stain CF 555
34 Antibody Labeling Kit and Mix-n-Stain CF 647 Antibody Labeling Kit (Sigma-Aldrich,
35 MX555S100 and MX647S100) were used according to the manufacturer's protocol.

36 Nanobodies equipped with an LPETGG motif and a His-tag at their C-terminus
37 were functionalized with triglycine containing probes using Sortase 5M as previously
38 described (Cheloha et al., 2019). Briefly, LPETGG motif and His-tag at the C-
39 terminus of nanobodies were replaced with fluorophore or biotin contained in
40 triglycine probes by sortagging reaction. Ni-NTA resin (EMD Millipore, 70691-3) was
41 used to remove unreacted His-tagged nanobodies and His-tagged Sortase 5M
42 enzyme, and the flow-through (sortase-based labeled nanobodies) was collected.
43 The flow-through was applied to PD-10 column (GE Healthcare, GE17-0851-01) to
44 remove excess triglycine probes.

1

2 **Immunostaining and imaging analysis**

3 *Drosophila* fat body and midguts from adult females were fixed in 4%
4 paraformaldehyde in Phosphate-buffered saline (PBS) at room temperature for 1
5 hour, incubated for 1 hour in Blocking Buffer (5% Normal Donkey Serum, 0.3% Triton
6 X-100, 0.1% Bovine serum albumin (BSA) in PBS), and stained with primary
7 antibodies overnight at 4°C in PBST (0.3% Triton X-100, 0.1% BSA in PBS). S2R+
8 cells were fixed in 4% paraformaldehyde in PBS at room temperature for 30 minutes,
9 incubated for 1 hour in Blocking Buffer, and stained with primary antibodies for 2-3
10 hours at room temperature in PBST. The primary antibodies and their dilutions used
11 are: NbVHH05-ALFA (1:500), NbVHH05-HA (1:500), NbVHH05-hlgG (1:20, S2 cell
12 culture media), NbVHH05-555 (1:500), Nb127D01-ALFA (1:500), Nb127D01-HA
13 (1:500), Nb127D01-hlgG (1:20, S2 cell culture media), Nb127D01-647 (1:500),
14 mouse anti-GFP (Invitrogen, A11120; 1:300), rat anti-HA (Sigma-Aldrich, 3F10;
15 1:1000). After primary antibody incubation, the fat body and midguts or S2R+ cells
16 were washed 3 times with PBST, stained with 4',6-diamidino-2-phenylindole (DAPI)
17 (1:2000 dilution) and Alexa Fluor-conjugated donkey-anti-mouse, donkey-anti-rabbit
18 and mouse-anti-human IgG secondary antibodies (Molecular Probes, 1:1000), or
19 NbALFA-Atto647 (NanoTag Biotechnologies, N1502-At647N-L; 1:500) Goat Anti-
20 Alpaca IgG-647 (Jackson ImmunoResearch, 128-605-230; 1:500) in PBST at 22°C
21 for 2 hours, washed 3 times with PBST, and mounted in Vectashield medium.

22 All images of the posterior midgut or S2R+ cells that are presented in this study
23 are confocal images captured with a Nikon Ti2 Spinning Disk confocal microscope.
24 Z-stacks of 5-20 images covering one layer of the epithelium from the apical to the
25 basal side were obtained, adjusted, and assembled using NIH Fiji (ImageJ), and
26 shown as a maximum projection.

27

28 **Western blots**

29 Cultured cells were harvested 3 days after transfection. For fly, 6-8 larval fat bodies
30 or 3 female midguts per group were dissected in PBS, placed in 50µl lysis buffer
31 (Pierce, #87788) with 2x protease and phosphatase inhibitor cocktail (Pierce,
32 #78440) and 2 mM trypsin inhibitor benzamidine (Sigma-Aldrich, #434760), and
33 homogenized using Kimble Kontes pellet pestles (Millipore, Z359947). Protein
34 lysates were incubated in 2xSDS sample buffer (Thermo Scientific, #39001)
35 containing 5% 2-Mercaptoethanol at 100°C for 10 minutes, ran on a 4%-20%
36 polyacrylamide gel (Bio-Rad, #4561096), and transferred to an Immobilon-P
37 polyvinylidene fluoride (PVDF) membrane (Millipore, IPVH00010). The membrane
38 was blocked by 5% BSA or 5% skim milk in 1x Tris-buffered saline (TBS) containing
39 0.1% Tween-20 (TBST) at room temperature for 30 minutes. The following primary
40 antibodies were used: anti-tubulin (Sigma, T5168, 1:10,000), rabbit anti-GFP
41 (Molecular Probes, A-6455; 1:10000) and anti-FLAG M1 (Sigma, F3040, 1:5,000), rat
42 anti-HA (Sigma-Aldrich, 3F10; 1:10000), NbVHH05 (0.2mg/ml, 1:5000, or
43 1:100~1:100000 used in concentration gradient test), Nb127D01 (0.2mg/ml, 1:5000,
44 or 1:100~1:100000 used in concentration gradient test), NbVHH05-hlgG (1:100, S2

1 cell culture media), Nb127D01-hIgG (1:100, S2 cell culture media) in blocking
2 solution. After washing with TBST, signals were detected with enhanced
3 chemiluminescence (ECL) reagents (Amersham, RPN2209; Pierce, #34095) or
4 fluorescent secondary antibody information. Western blot images were acquired by
5 Bio-Rad ChemiDoc MP or X-ray film exposure.

6 7 **Immunoprecipitation**

8 For immunoprecipitation using ALFA-tagged nanobodies (NbVHH05-ALFA and
9 Nb127D01-ALFA), His-tag purified nanobodies from bacteria were incubated with
10 ALFA Selector ST resin (Nanotag Biotechnologies, N1511) at room temperature for 1
11 hour. The resin was washed with Pierce IP lysis buffer (Thermo Scientific, 87787)
12 (3X) and incubated with S2 cell culture media containing secreted GFP proteins with
13 3xVHH05-tag and 3x127D01-tag at 4°C for 1 hour. After washing in IP lysis buffer
14 (4X), proteins were eluted in 2x sample buffer.

15 For immunoprecipitation using human IgG-formatted nanobody (Nb127D01-
16 hIgG), Protein A Magnetic Beads (Bio-Rad, 1614013) were incubated with S2 cell
17 culture media containing Nb127D01-hIgG at room temperature for 1 hour. After
18 washing in IP lysis buffer (3X), beads were incubated with the conditioned media
19 containing secreted GFP proteins 3x127D01-tag at 4°C for 1 hour. After washing in
20 IP lysis buffer (4X), proteins were eluted in 2x sample buffer.

21 22 **ELISA**

23 GFP fused at its C-terminus with a peptide corresponding to the extracellular portion
24 of human CXCR2 (full-length, Supplementary Figure 1), produced through
25 sortagging, was immobilized on Nunc 96-well Maxisorp flat bottom plates (100
26 ng/well). After immobilization, wells were blocked using a solution of BSA in PBS (5%
27 w/v). Nb127D01 conjugated with biotin (20 nM) was mixed with peptides
28 corresponding to full-length CXCR2 extracellular domain or two fragments at varying
29 concentrations. These solutions were then added to plates with immobilized GFP-
30 CXCR2 and incubated for 1 h. These solutions were discarded from the plates, the
31 plates were washed with PBS containing 0.05% Tween-20, and the amount of
32 Nb127D01-biotin bound to the plate was quantified through the addition of
33 streptavidin-HRP (Thermo Fisher, N100), washing, and the addition of
34 tetramethylbenzidine-containing solution (Thermo Fisher, N301).

35 **Trehalose assay**

36 Whole-body trehalose levels were measured from 5-6 groups (each group has 4
37 female flies). Fly samples were homogenized with 300ul TBST buffer (5 mM Tris-HCl
38 [pH 6.6], 137 mM NaCl, 2.7 mM KCl, 0.1% TritonX-100), heated at 75 °C for 10min,
39 and centrifuged at 3000 g for 1 min. 10 ul of supernatant was added to 100ul glucose
40 assay reagent (Megazyme; K-GLUC) with or without trehalose (1:500; Megazyme; E-
41 TREH) at 37 °C for 30 min. The absorbance at 340 nm was measured on a
42 Molecular Devices SpectraMax Paradigm plate reader. The trehalose concentration

1 in the sample was determined by subtracting the glucose concentration from the total
2 sugar concentration.

3

4 **Acknowledgements**

5 We thank the assistance provided by the Microscopy Resources on the North Quad
6 (MicRoN) core at Harvard Medical School and Christians Villalta for help with the
7 generation of transgenic flies. We thank Seung K. Kim for providing the Dilp2
8 antibody. This work was supported by NIH NIGMS P41 GM132087. A.K is supported
9 by Postdoctoral Fellowship Program (Nurturing Next-generation Researchers)
10 through the National Research Foundation of Korea (NRF) funded by the Ministry of
11 Education (2021R1A6A3A14039622). J.S.S. L. is supported by a Croucher fellowship
12 for Postdoctoral Research from the Croucher Foundation. N.P. is an investigator of
13 Howard Hughes Medical Institute.

14 **Additional information**

15 **Author contributions**

16 J.X., A.R. K. and N.P. conceptualized and designed the experiments. J.X. and A.R.
17 K. performed most of the experiments. R.W. C., F.A. F., H. P., J.S.S. L., Y. F., E. S.
18 and R. B. contributed reagents and helped with experiments. J.X., A.R. K., R. W. C.
19 and N.P. analyzed the data. J.X. and A.R. K. wrote the paper (original draft). J.S.S.
20 L., S.E. M., J. Z., R. W. C., H. P. and N.P. edited the paper. All authors discussed the
21 results and commented on the paper.

22

23 **References**

24 Aguilar G, Matsuda S, Vigano MA, Affolter M. 2019. Using Nanobodies to Study Protein
25 Function in Developing Organisms. *Antibodies (Basel)* **8**: 16.

26 Anzalone AV, Randolph PB, Davis JR, Sousa AA, Koblan LW, Levy JM, Chen PJ, Wilson C,
27 Newby GA, Raguram A, Liu DR. 2019. Search-and-replace genome editing without double-
28 strand breaks or donor DNA. *Nature* **576**: 149–157.

29 Boersma S, Khuperkar D, Verhagen BMP, Sonneveld S, Grimm JB, Lavis LD, Tanenbaum
30 M.E. 2019. Multi-Color Single-Molecule Imaging Uncovers Extensive Heterogeneity in mRNA
31 Decoding. *Cell* **178**: 458–472.

32 Bosch JA, Birchak G, Perrimon N. 2021. Precise genome engineering in Drosophila using
33 prime editing. *PNAS* **118**: e2021996118.

- 1 Bradley ME, Dombrecht B, Manini J, Willis J, Vlerick D, De Taeye S, Van den Heede K,
2 Roobrouck A, Grot E, Kent TC, Laeremans T, Steffensen S, Van Heeke G, Brown Z, Charlton
3 SJ, Cromie KD. 2015. Potent and efficacious inhibition of CXCR2 signaling by biparatopic
4 nanobodies combining two distinct modes of action. *Molecular Pharmacology* **87**: 251–262.
- 5 Broughton S, Alic N, Slack C, Bass T, Ikeya T, Vinti G, Tommasi AM, Driège Y, Hafen E,
6 Partridge L. 2008. Reduction of DILP2 in *Drosophila* triages a metabolic phenotype from
7 lifespan revealing redundancy and compensation among DILPs. *PLoS One* **3**: e3721.
- 8 Caussinus E, Affolter M. 2016. deGradFP: A System to Knockdown GFP-Tagged Proteins.
9 *Methods in Molecular Biology* **1478**: 177–187.
- 10 Caussinus E, Kanca O, Affolter M. 2011. Fluorescent fusion protein knockout mediated by
11 anti-GFP nanobody. *Nature Structural & Molecular Biology* **9**: 117–121.
- 12 Cheloha RW, Harmand TJ, Wijne C, Schwartz TU, Ploegh HL. 2020. Exploring cellular
13 biochemistry with nanobodies. *Journal of Biological Chemistry* **295**: 15307–15327.
- 14 Cheloha RW, Li Z, Bousbaine D, Woodham AW, Perrin P, Volarić J, Ploegh HL. 2019.
15 Internalization of Influenza Virus and Cell Surface Proteins Monitored by Site-Specific
16 Conjugation of Protease-Sensitive Probes. *ACS Chemical Biology* **14**: 1836–1844.
- 17 De Genst EJ, Guilliams T, Wellens J, O'Day EM, Waudby CA, Meehan S, Dumoulin M, Hsu ST,
18 Cremades N, Verschueren KH, Pardon E, Wyns L, Steyaert J, Christodoulou J, Dobson CM.
19 2010. Structure and properties of a complex of α -synuclein and a single-domain camelid
20 antibody. *Journal of Molecular Biology* **402**: 326–343.
- 21 Fang T, Lu X, Berger D, Gmeiner C, Cho J, Schalek R, Ploegh H, Lichtman J. 2018.
22 Nanobody immunostaining for correlated light and electron microscopy with preservation of
23 ultrastructure. *Nature Methods* **15**: 1029–1032.
- 24 Fornasiero EF, Opazo F. 2015. Super-resolution imaging for cell biologists: concepts,
25 applications, current challenges and developments. *Bioessays* **37**: 436–451.
- 26 Götzke H, Kilisch M, Martínez-Carranza M, Sograte-Idrissi S, Rajavel A, Schlichthaerle T,
27 Engels N, Jungmann R, Stenmark P, Opazo F, Frey S. 2019. The ALFA-tag is a highly
28 versatile tool for nanobody-based bioscience applications. *Nature Communications* **10**: 4403.
- 29 Guimaraes CP, Witte MD, Theile CS, Bozkurt G, Kundrat L, Blom AE, Ploegh HL. 2013. Site-
30 specific C-terminal and internal loop labeling of proteins using sortase-mediated reactions.
31 *Nature Protocols* **8**: 1787–1799.
- 32 Harmansa S, Alborelli I, Bieli D, Caussinus E, Affolter M. 2017. A nanobody-based toolset to
33 investigate the role of protein localization and dispersal in *Drosophila*. *Elife* **6**: e22549.

- 1 Harmansa S, Affolter M. 2018. Protein binders and their applications in developmental
2 biology. *Development* **145**: dev148874.
- 3 Helma J, Cardoso MC, Muyldermans S, Leonhardt H. 2015. Nanobodies and recombinant
4 binders in cell biology. *Journal of Cell Biology* **209**: 633–644.
- 5 Harmansa S, Hamaratoglu F, Affolter M, Caussinus E. 2015. Dpp spreading is required for
6 medial but not for lateral wing disc growth. *Nature* **527**: 317–322.
- 7 Lamb AM, Walker EA, Wittkopp PJ. 2017. Tools and strategies for scarless allele replacement
8 in *Drosophila* using CRISPR/Cas9. *Fly (Austin)* **11**: 53–64.
- 9 Ling J, Cheloha RW, McCaul N, Sun ZJ, Wagner G, Ploegh HL. 2019. A nanobody that
10 recognizes a 14-residue peptide epitope in the E2 ubiquitin-conjugating enzyme UBC6e
11 modulates its activity. *Molecular Immunology* **114**: 513–523.
- 12 Ling L, Kokoza VA, Zhang C, Aksoy E, Raikhe AS. 2017. MicroRNA-277 targets insulin-like
13 peptides 7 and 8 to control lipid metabolism and reproduction in *Aedes aegypti* mosquitoes.
14 *PNAS* **114**: E8017–E8024.
- 15 Li-Kroeger D, Kanca O, Lee PT, Cowan S, Lee MT, Jaiswal M, Salazar JL, He Y, Zuo Z,
16 Bellen HJ. 2018. An expanded toolkit for gene tagging based on MiMIC and scarless CRISPR
17 tagging in *Drosophila*. *Elife* **7**: e38709.
- 18 Mikhaylova M, Cloin BM, Finan K, van den Berg R, Teeuw J, Kijanka MM, Sokolowski M,
19 Katrukha EA, Maidorn M, Opazo F, Moutel S, Vantard M, Perez F, van Bergen en
20 Henegouwen PM, Hoogenraad CC, Ewers H, Kapitein LC. 2015. Resolving bundled
21 microtubules using anti-tubulin nanobodies. *Nature Communications* **6**: 7933.
- 22 Mohr SE, Tattikota SG, Xu J, Zirin J, Hu Y, Perrimon N. 2021. Methods and tools for spatial
23 mapping of single-cell RNAseq clusters in *Drosophila*. *Genetics* **217**: iyab019.
- 24 Morin X, Daneman R, Zavortink M, Chia W. 2001. A protein trap strategy to detect GFP-
25 tagged proteins expressed from their endogenous loci in *Drosophila*. *PNAS* **98**: 15050–
26 15055.
- 27 Neumüller RA, Wirtz-Peitz F, Lee S, Kwon Y, Buckner M, Hoskins RA, Venken KJ, Bellen HJ,
28 Mohr SE, Perrimon, N. 2012. Stringent analysis of gene function and protein-protein
29 interactions using fluorescently tagged genes. *Genetics* **190**: 931–940.
- 30 Park S, Alfa RW, Topper SM, Kim GE, Kockel L, Kim SK. 2014. A genetic strategy to measure
31 circulating *Drosophila* insulin reveals genes regulating insulin production and secretion. *PLoS*
32 *Genetics* **10**: e1004555.
- 33 Sarov M, Barz C, Jambor H, Hein MY, Schmied C, Suchold D, Stender B, Janosch S, K J VV,
34 Krishnan RT, Krishnamoorthy A, Ferreira IR, Ejsmont RK, Finkl K, Hasse S, Kämpfer P,

- 1 Plewka N, Vinis E, Schloissnig S, Knust E, Hartenstein V, Mann M, Ramaswami M,
2 VijayRaghavan K, Tomancak P, Schnorrer F. (2016). A genome-wide resource for the analysis
3 of protein localisation in *Drosophila*. *Elife* **5**: e12068.
- 4 Tanenbaum ME, Gilbert LA, Qi LS, Weissman JS, Vale RD. 2014. A protein-tagging system
5 for signal amplification in gene expression and fluorescence imaging. *Cell* **159**: 635–646.
- 6 Tiebe M, Lutz M, De La Garza A, Buechling T, Boutros M, Teleman AA. 2015. REPTOR and
7 REPTOR-BP Regulate Organismal Metabolism and Transcription Downstream of TORC1.
8 *Developmental Cell* **33**: 272–284.
- 9 Traenkle B, Emele F, Anton R, Poetz O, Haeussler RS, Maier J, Kaiser PD, Scholz AM,
10 Nueske S, Buchfellner A, Romer T, Rothbauer U. 2015. Monitoring interactions and dynamics
11 of endogenous beta-catenin with intracellular nanobodies in living cells. *Molecular & Cellular
12 Proteomics* **14**: 707–723.
- 13 Vigano MA, Ell CM, Kustermann MMM, Aguilar G, Matsuda S, Zhao N, Stasevich TJ, Affolter
14 M, Pyrowolakis G. 2021. Protein manipulation using single copies of short peptide tags in
15 cultured cells and in *Drosophila melanogaster*. *Development* **148**: dev191700.
- 16 Virant D, Traenkle B, Maier J, Kaiser PD, Bodenhöfer M, Schmees C, Vojnovic I, Pisak-
17 Lukáts B, Endesfelder U, Rothbauer U. 2018. A peptide tag-specific nanobody enables high-
18 quality labeling for dSTORM imaging. *Nature Communications* **9**: 930.
- 19 Wang S, Tang NH, Lara-Gonzalez P, Zhao Z, Cheerambathur DK, Prevo B, Chisholm AD,
20 Desai A, Oegema K. 2017. A toolkit for GFP-mediated tissue-specific protein degradation in
21 *C. elegans*. *Development* **44**: 2694–2701.
- 22 Xu J, Liu W, Yang D, Chen S, Chen K, Liu Z, Yang X, Meng J, Zhu G, Dong S, Zhang Y, Zhan
23 S, Wang G, Huang Y. 2020. Regulation of olfactory-based sex behaviors in the silkworm by
24 genes in the sex-determination cascade. *PLoS Genetics* **16**: e1008622.
- 25 Yamaguchi N, Colak-Champollion T, Knaut H. 2019. zGrad is a nanobody-based degron
26 system that inactivates proteins in zebrafish. *Elife* **8**: e43125.
- 27 Zhao N, Kamijo K, Fox PD, Oda H, Morisaki T, Sato Y, Kimura H, Stasevich TJ. 2019. A
28 genetically encoded probe for imaging nascent and mature HA-tagged proteins in vivo.
29 *Nature Communications* **10**: 2947.

30
31

32 **Figure legends**

33 **Figure 1.** VHH05 and 127D01 NanoTag sequences and their corresponding
34 nanobodies, and use of nanobodies as chromobodies. **(A and C)** VHH05 and
35 127D01 were inserted at the N-terminus, internally or at the C-terminus of a protein
36 of interest (POI). GSG denotes the linker, M is the start codon, and Stop is the stop

1 codon. **(B and D)** Nanobody sequences of NbVHH05 and Nb127D01. Bolded and
2 underlined CDR1-3 correspond to complementarity-determining regions (CDRs). **(E)**
3 Co-transfection of pAW-actin5C-NbVHH05-GFP and pAW-actin5C-VHH05-H2B-
4 mCherry into S2R+ cells. H2B is a nuclear protein. **(F)** Co-transfection of pAW-
5 actin5C-NbVHH05-GFP and pAW-actin5C-CD8-VHH05-mCherry into S2R+ cells.
6 CD8 is a cell membrane protein **(G)** Co-transfection of pAW-actin5C-NbVHH05-GFP
7 and pAW-actin5C-mito-mCherry-VHH05 into S2R+ cells. Mito-mCherry-VHH05
8 contains a localization signal peptide for mitochondrial outer membrane targeting. **(H,**
9 **I and J)** Experiments are as in E, F and G, except that pAW-actin5C-Nb127D01-GFP
10 and pAW-actin5C-127D01-H2B-mCherry were co-transfected.

11

12 **Figure 2.** Using NbVHH05 and Nb127D01 for immunofluorescence. **(A)** Fluorophore-
13 conjugated NbVHH05 or Nb127D01 recognizes VHH05- or 127D01-tagged
14 fluorescence proteins. **(A')** VHH05- or 127D01-tagged mito-GFP can be detected by
15 the corresponding NbVHH05-555 or Nb127D01-647 in transfected S2R+ cells. **(B)**
16 Schematic of nanobodies containing ALFA-tag as primary antibody and NbALFA as a
17 secondary antibody. **(B')** VHH05- or 127D01-tagged mito-GFP can be detected using
18 the corresponding nanobodies in transfected S2R+ cells. **(C)** Schematic of
19 fluorophore-conjugated anti-Alpaca IgG antibodies to detect VHH05- and 127D01-
20 tagged proteins. NbVHH05 or Nb127D01 are used as primary antibodies and anti-
21 Alpaca IgG as secondary antibody. **(C')** VHH05- or 127D01-tagged mito-GFP can be
22 detected using the corresponding nanobodies and anti-Alpaca IgG-647 in transfected
23 S2R+ cells. **(D)** Schematic of using VHH05 and 127D01 for double tagging. N-, C-
24 terminal of REPTOR contains VHH05 and 127D01. **(D')** Co-straining NbVHH05 and
25 Nb127D01 in S2R+ cells transfected with VHH05-REPTOR-127D01. Scale bars: 10
26 μm .

27

28 **Figure 3.** Detection of tagged target proteins by western blotting and
29 immunoprecipitation. **(A)** Lysates from S2R+ cells, transfected with different tagged
30 plasmids (as used in Figure 1) or a mock control plasmid, were analyzed by SDS-
31 PAGE and western blotting. The blot was developed with NbVHH05 and Nb127D01
32 followed by NbALFA-HRP or a mouse anti-tubulin primary antibody followed by anti-
33 Mouse IgG HRP. **(B)** Schematics depict VHH05- or 127D01-tagged secreted GFP
34 proteins bound by NbVHH05-ALFA and Nb127D01-ALFA followed by NbALFA-HRP.
35 Culture media from S2R+ cells transfected with secreted BiP-GFP-1xtag, BiP-GFP-
36 2xtag, BiP-GFP-3xtag were used for the western blotting. Anti-FLAG antibody was
37 used to show the GFP level. Histogram showing the relative gray value of anti-
38 NbVHH05 or anti-Nb127D01 to anti-FLAG. Plasmid information is in Supplementary
39 Fig. 6. **(C)** Western blots for S2R+ cell culture media containing Upd2 double-tagged
40 protein: N- and C-terminus region of Upd2 contains VHH05 and 127D01,
41 respectively, recognized by NbVHH05 or Nb127D01. The secondary antibodies were
42 anti-HiIgG-HRP, anti-ALFA-800, and Streptavidin-800. **(D)** Immunoprecipitation of
43 FLAG-GFP-3xVHH05 using NbVHH05-ALFA and ALFA-resin. The control nanobody
44 failed to capture FLAG-GFP-3xVHH05. **(E)** Immunoprecipitation of FLAG-GFP-

1 3x127D01 using Nb127D01-ALFA and ALFA-resin. (F) Immunoprecipitation of
2 FLAG-GFP-3x127D01 using Nb127D01-hIgG and Protein A magnetic bead.

3

4 **Figure 4.** Nanobody-based system for altering localization of NanoTagged proteins.
5 (A and B) Diagram showing the vectors used for the secreted protein trapping
6 method. NbVHH05/Nb127D01 fused to mCherry contains KDEL and BiP signal
7 peptide and is driven by the actin5C promoter. (C) Four independent cell transfection
8 experiments were performed. In 1 and 3, only GFP-VHH05 or GFP-127D01 was
9 transfected. In 2 and 4, NbVHH05-mCherry-KDEL with GFP-VHH05, or Nb127D01-
10 mCherry-KDEL with GFP-127D01, were co-transfected. Images show the GFP and
11 mCherry signal 48 hours after transfection. Nuclei are stained with DAPI. (D)
12 Immunoblots of GFP and tubulin in cell lysates from transfections 1-4.

13

14 **Figure 5.** Nanobodies expression *in vivo*. (A-D) *Lpp-Gal4* drives fat body expression
15 of *UAS-NbVHH05-GFP*, *UAS-NbVHH05-HA*, *UAS-Nb127D01-GFP*, or *UAS-*
16 *Nb127D01-HA*, detected by GFP or anti-HA immunostaining. (E and F) Western blot
17 detection of cytoplasmic and secreted GFP- or HA-tagged nanobodies. Lysates from
18 fat body or hemolymph were tested by anti-GFP, anti-HA and anti-tubulin antibodies.
19 Cytoplasmic-expressed nanobodies: *UAS-NbVHH05-GFP*, *UAS-Nb127D01-GFP*,
20 *UAS-NbVHH05-HA* and *UAS-Nb127D01-HA*. Secreted-expressed nanobodies: *UAS-*
21 *BiP-NbVHH05-GFP*, *UAS-BiP-Nb127D01-GFP*, *UAS-BiP-NbVHH05-HA* and *UAS-*
22 *BiP-Nb127D01-HA*. (G-J) Confocal images of *Drosophila* adult guts expressing
23 127D01-EGFP/VHH05-GFP and VHH05-REPTOR-127D01 with or without
24 rapamycin (Rapa) treatment for 15 hours. REPTOR shuttles into the nucleus upon
25 Rapa treatment. G and I as controls only express 127D01-EGFP or VHH05-GFP in
26 the ECs. H combines 127D01-EGFP with VHH05-REPTOR-127D01 and J combines
27 VHH05-EGFP with VHH05-REPTOR-127D01.

28

29 **Figure 6.** Integration of *3x127D01* into *Dilp2* shows a robust expression pattern in
30 the brain. (A) Workflow and schematic representation of the *Dilp2* gene and the
31 sgRNA targeting site. (B) PCR amplification was used to confirm the insertion. (C)
32 Representative sequencing chromatogram of PCR products from the junction PCR.
33 (D) Sequencing results of the DNA fragments showing 3x tag genome-donor
34 integration. (E) Larval brains of *w1118* and *Dilp2-3x127D01* co-stained with Dilp2
35 antibody and Nb127D01. Box demarcates Dilp2-expressing cells and Dilp2-positive
36 neuronal projections. (F) Measurement of whole body trehalose concentration in *y,w*
37 and *y,w; Dilp2-3x127D01* flies. (G) Nanobody immunostaining showing different Dilp2
38 expression after starvation. Red outline demarcates Dilp2-expressing cells and white
39 outline demarcates Dilp2-positive neuronal projections. Scale bars: 100 μ m.

40

41

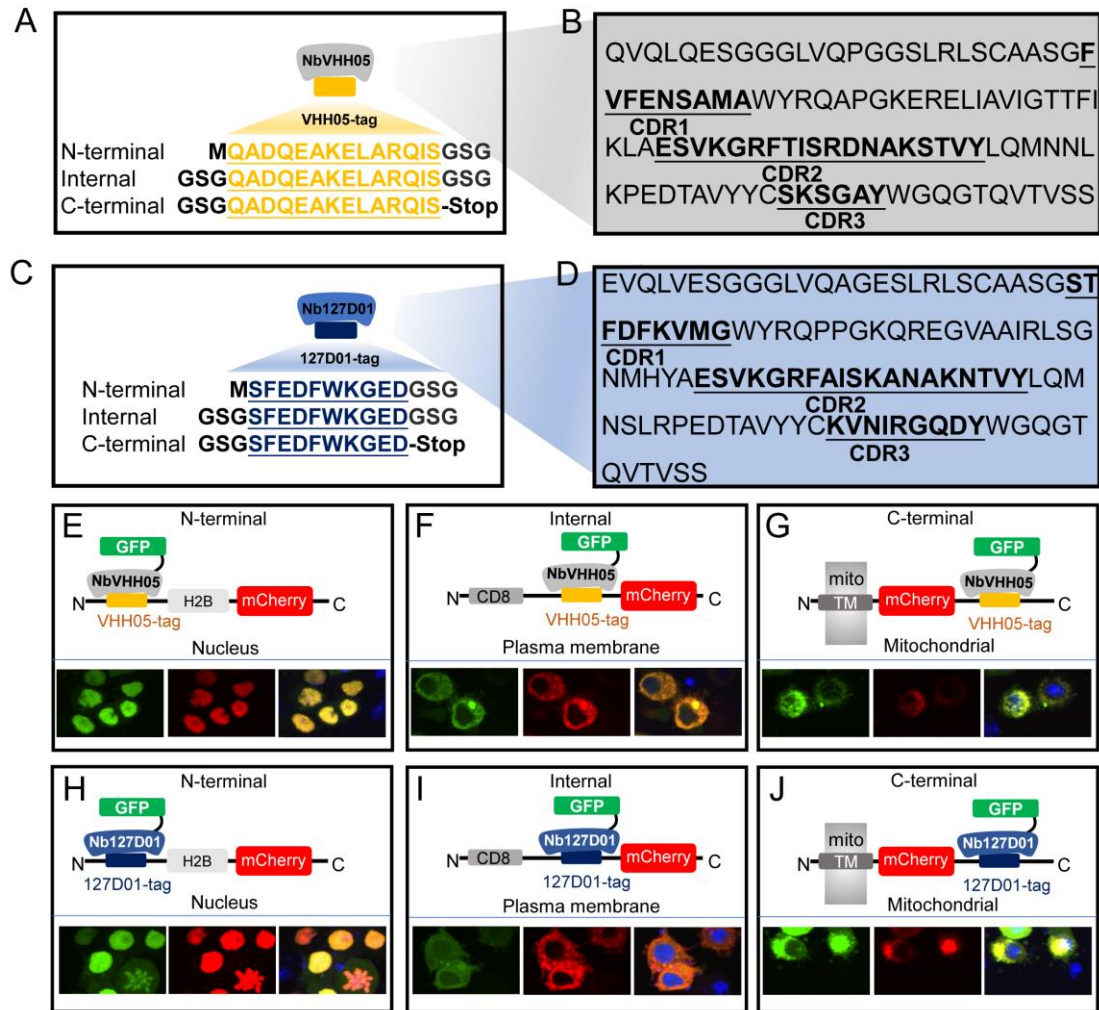
42

43

44

1 **Figure 1**

2



3

4

5

6

7

8

9

10

11

12

13

14

15

16

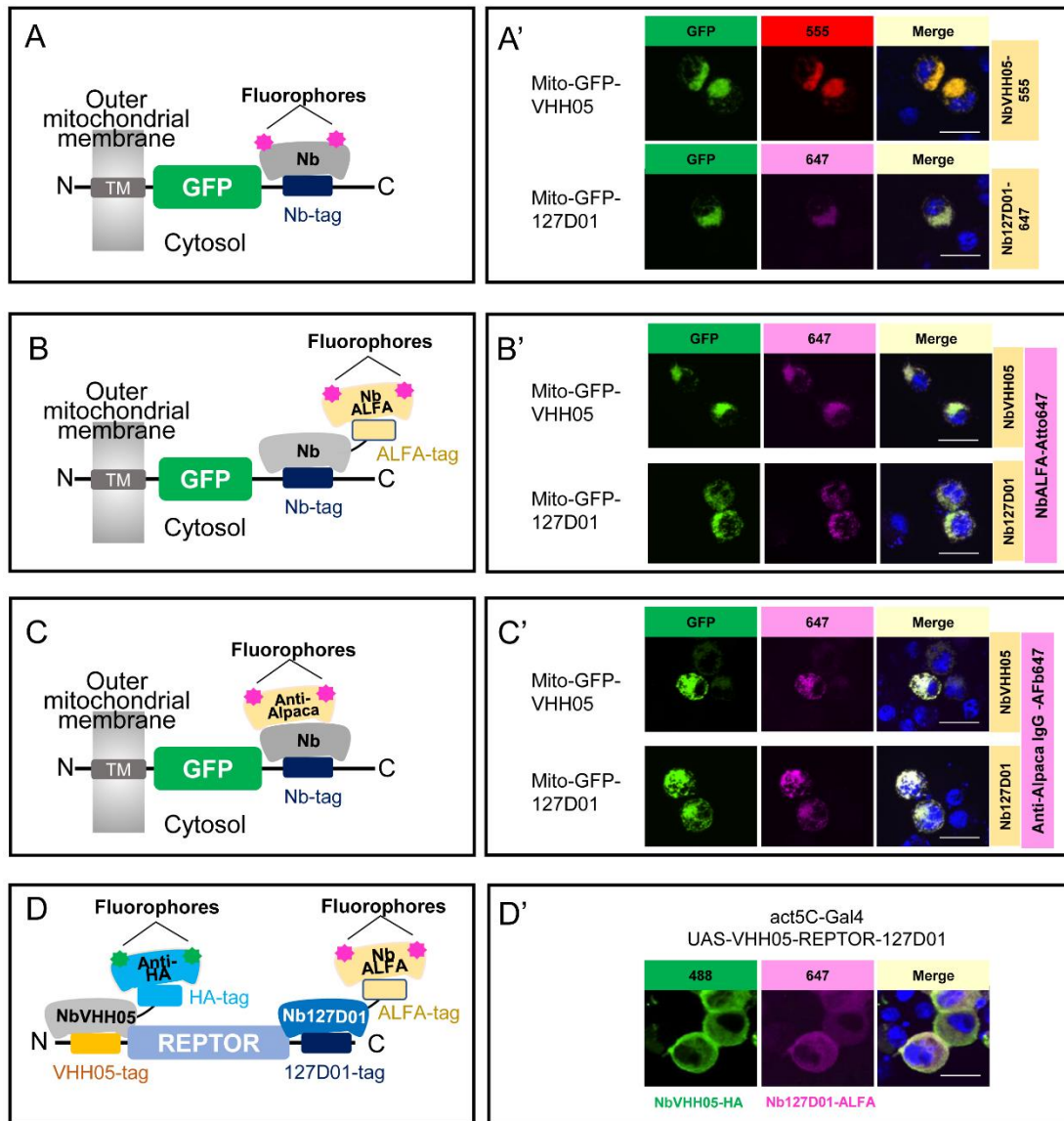
17

18

19

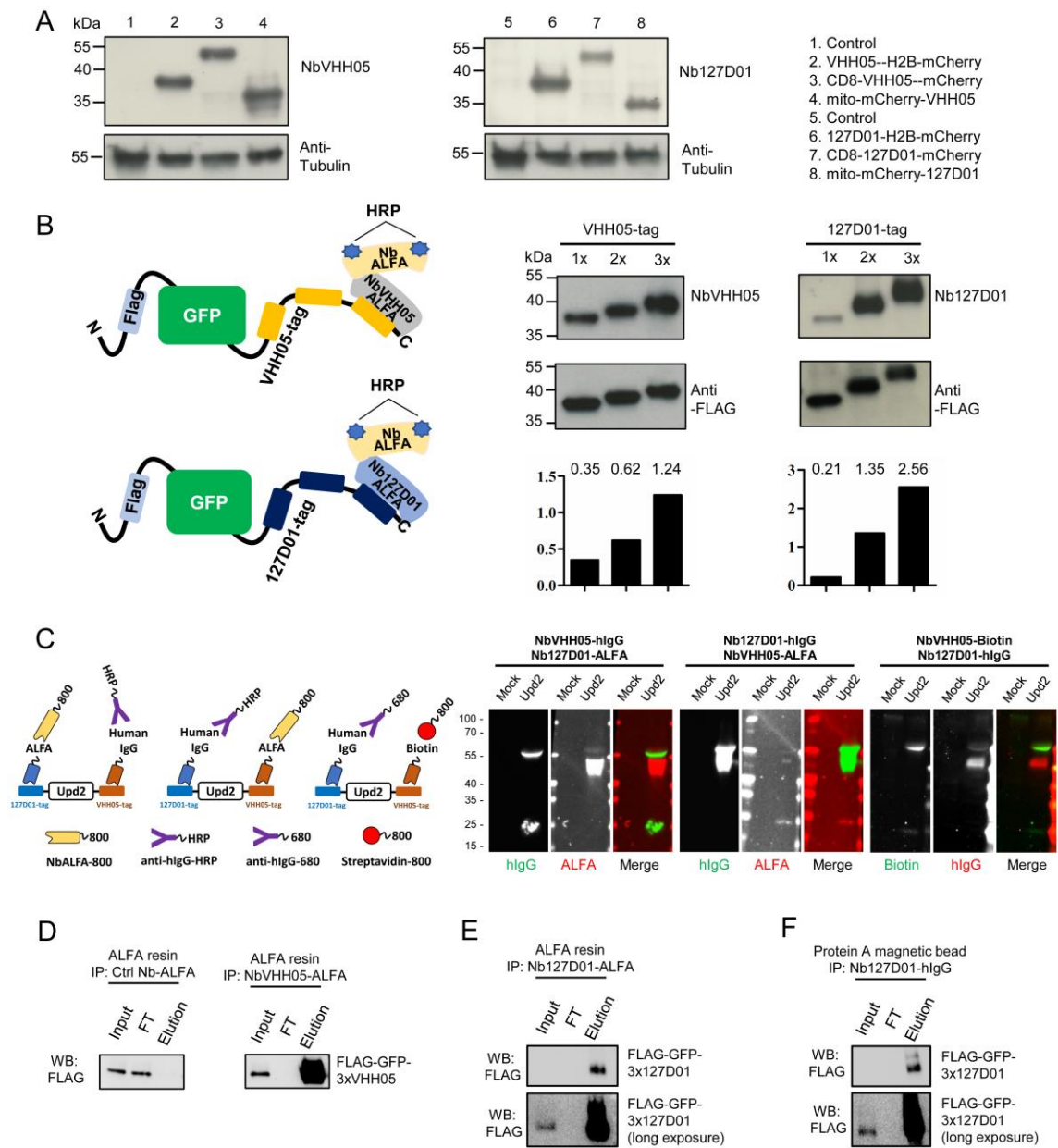
20

1 **Figure 2**



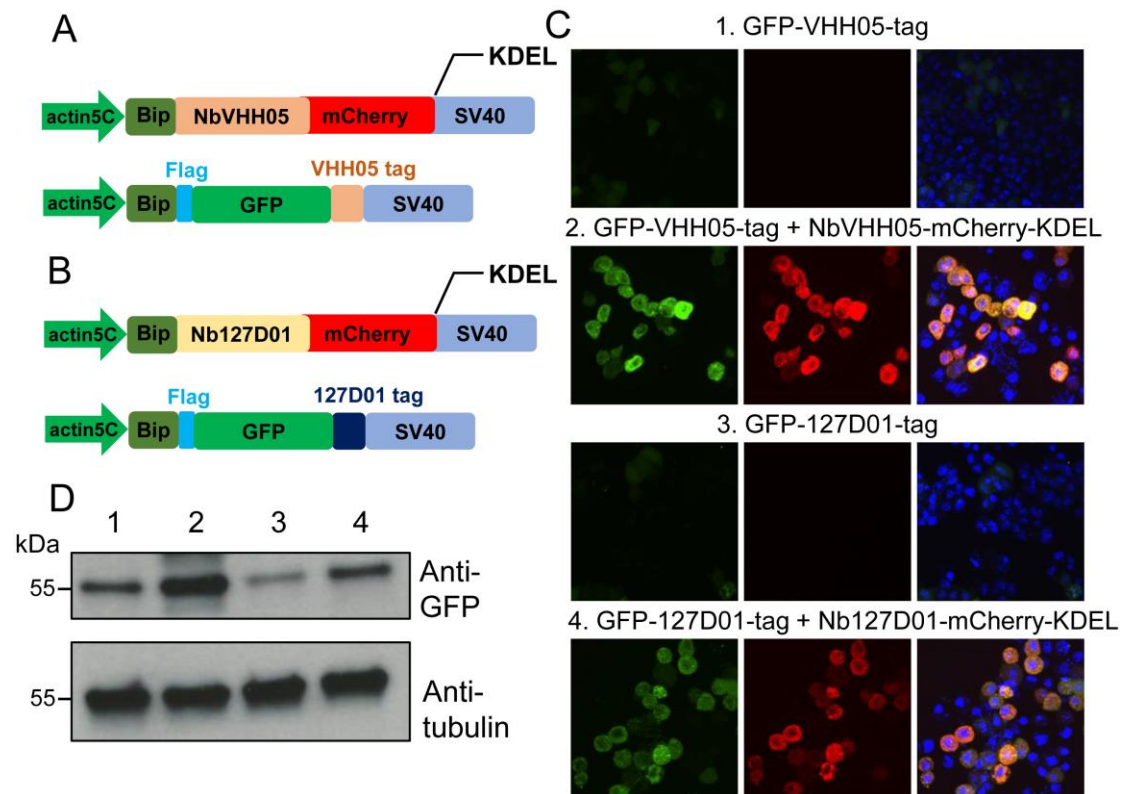
2
3
4

1 **Figure 3**



1 **Figure 4**

2



3

4

5

6

7

8

9

10

11

12

13

14

15

16

17

18

19

20

21

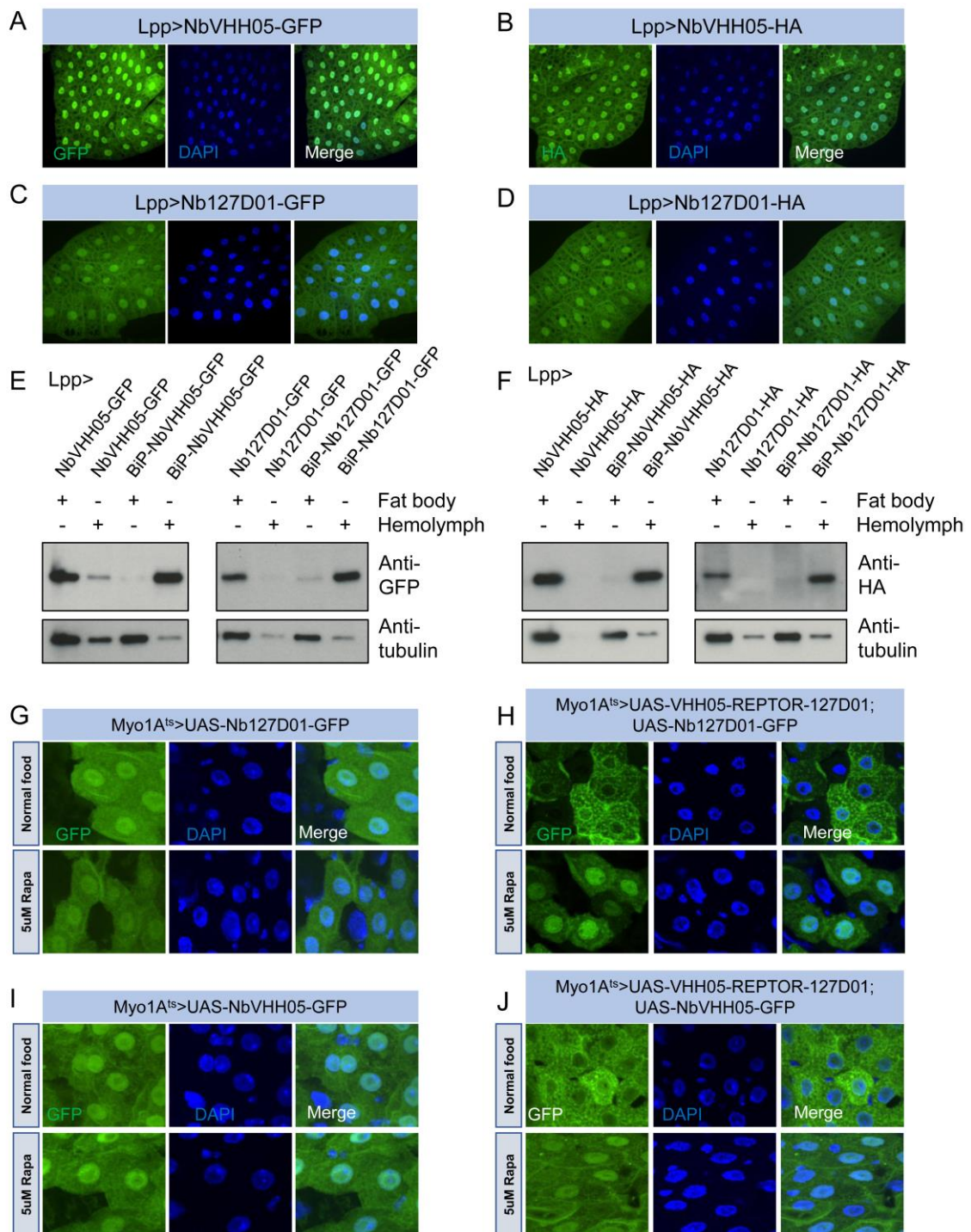
22

23

24

25

1 **Figure 5**



2

3

4

5

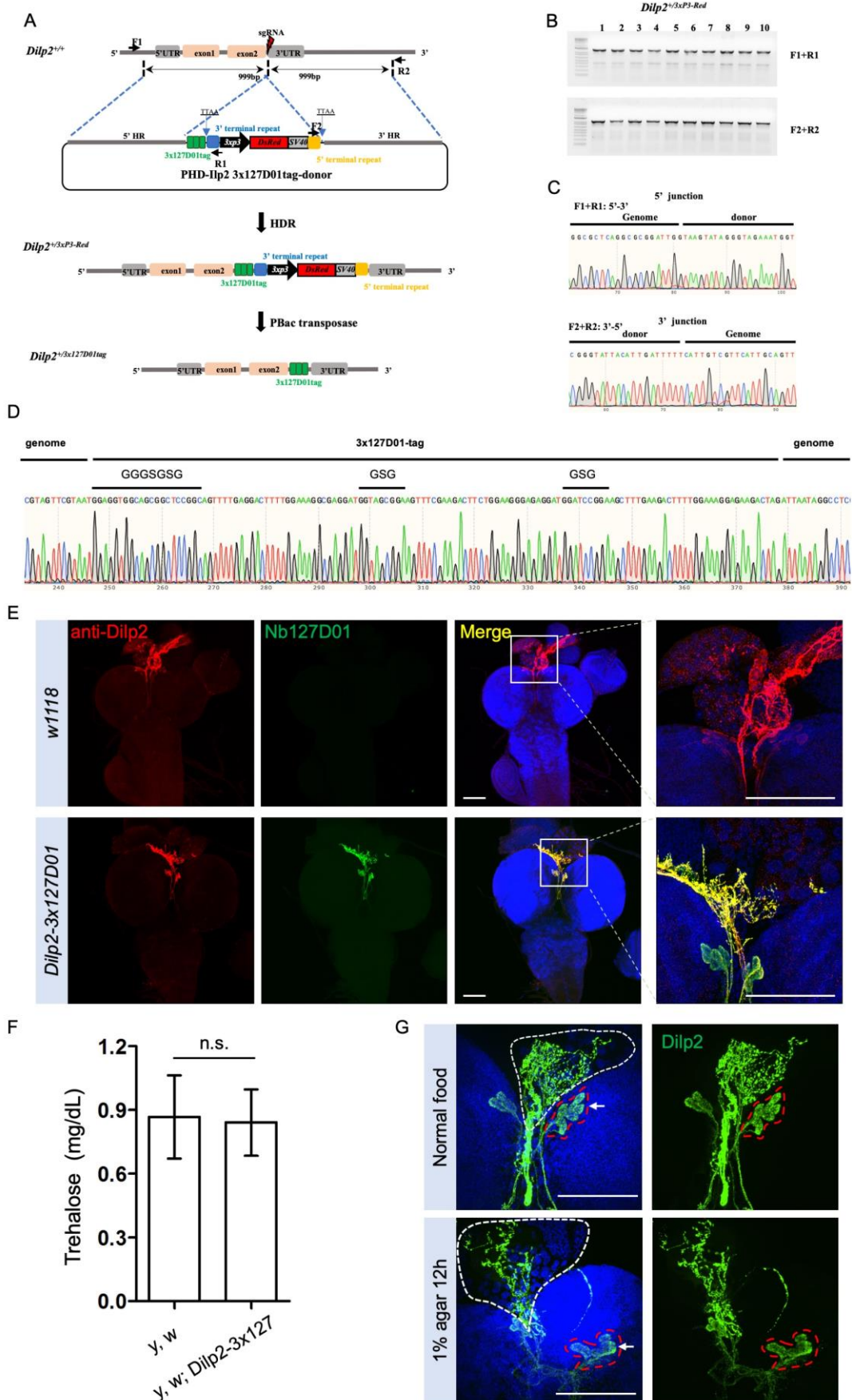
6

7

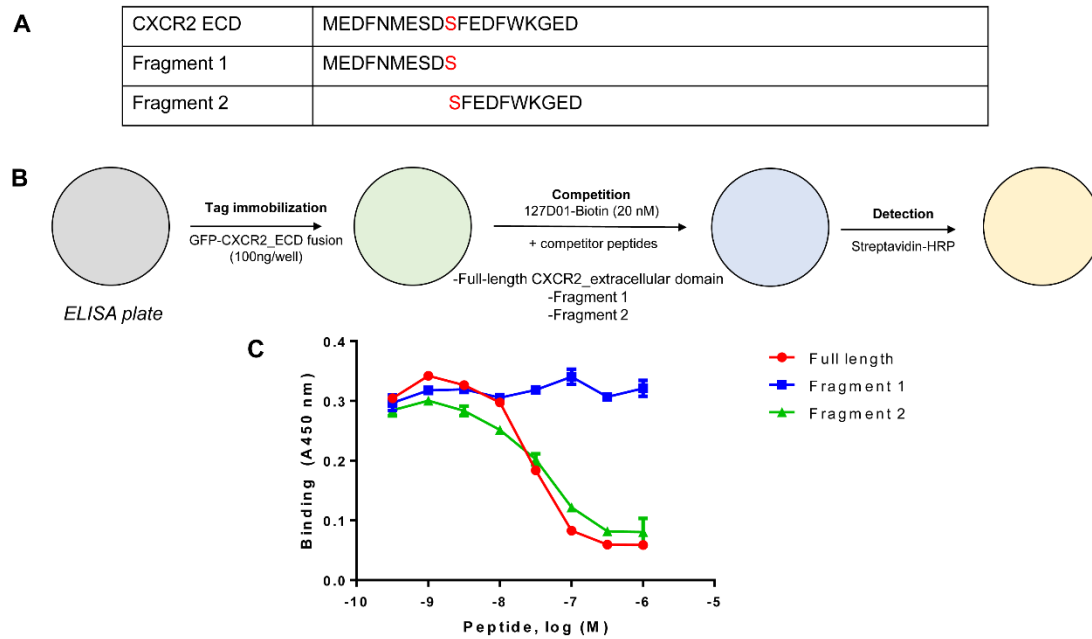
8

9

1 **Figure 6**



1 Supplemental Information



2

3 **Figure 1—figure supplement 1.** Identification of the 127D01 epitope. **(A)** Synthetic
4 peptides corresponding to the full-length extracellular domain from CXCR2 or
5 fragments were synthesized by solid-phase peptide synthesis using Fmoc protection
6 of the peptide backbone and purified by reverse-phase HPLC. **(B)** Peptides were used
7 in a competitive ELISA in which soluble peptides compete for binding with a conjugate
8 consisting of GFP fused with CXCR2 ECD immobilized on the ELISA plate. **(C)**
9 Representative data from a competition ELISA experiment. Data points represent
10 mean \pm SD from duplicate experiments.

11

12

13

14

15

16

17

18

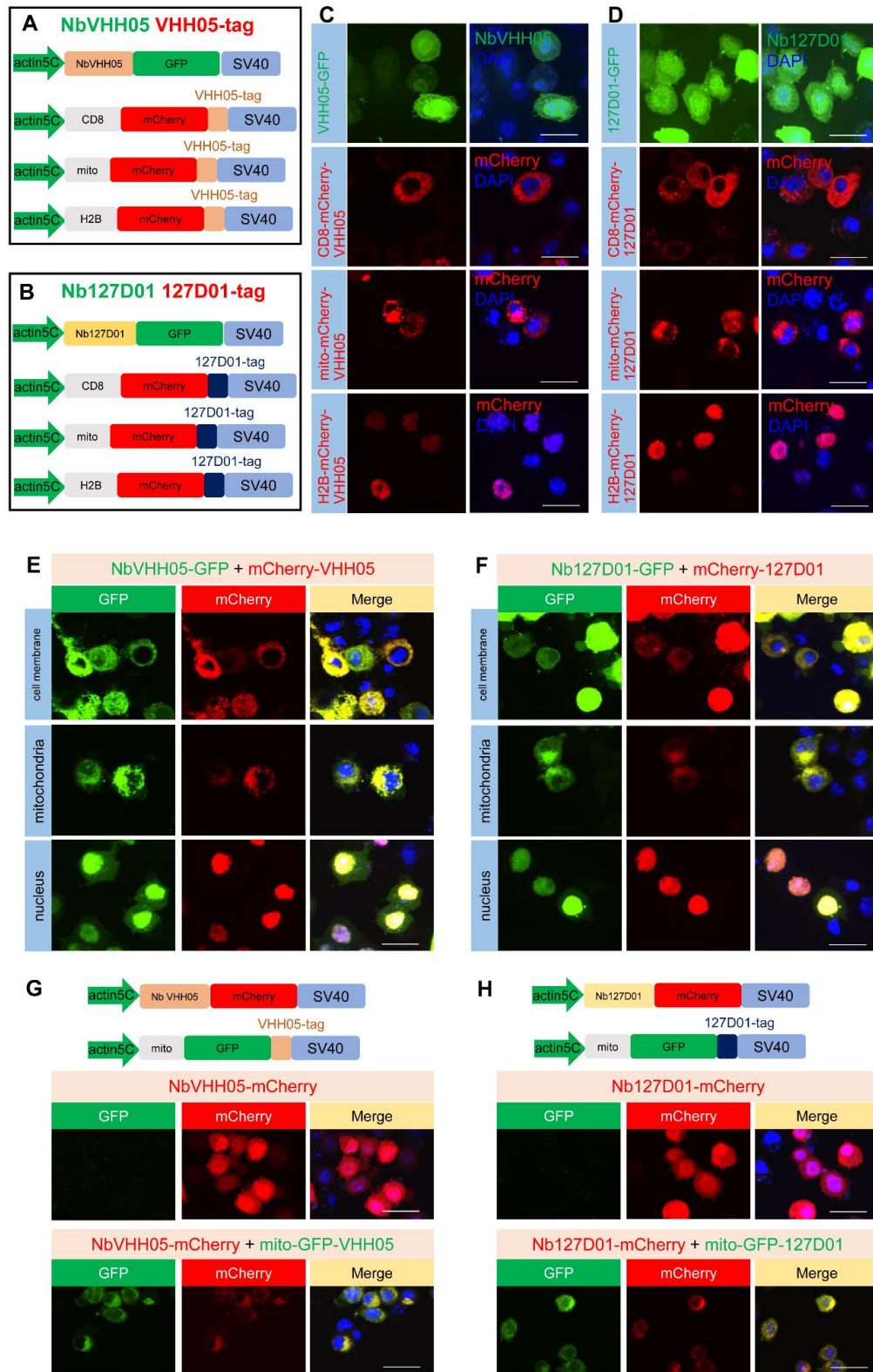
19

20

21

22

23

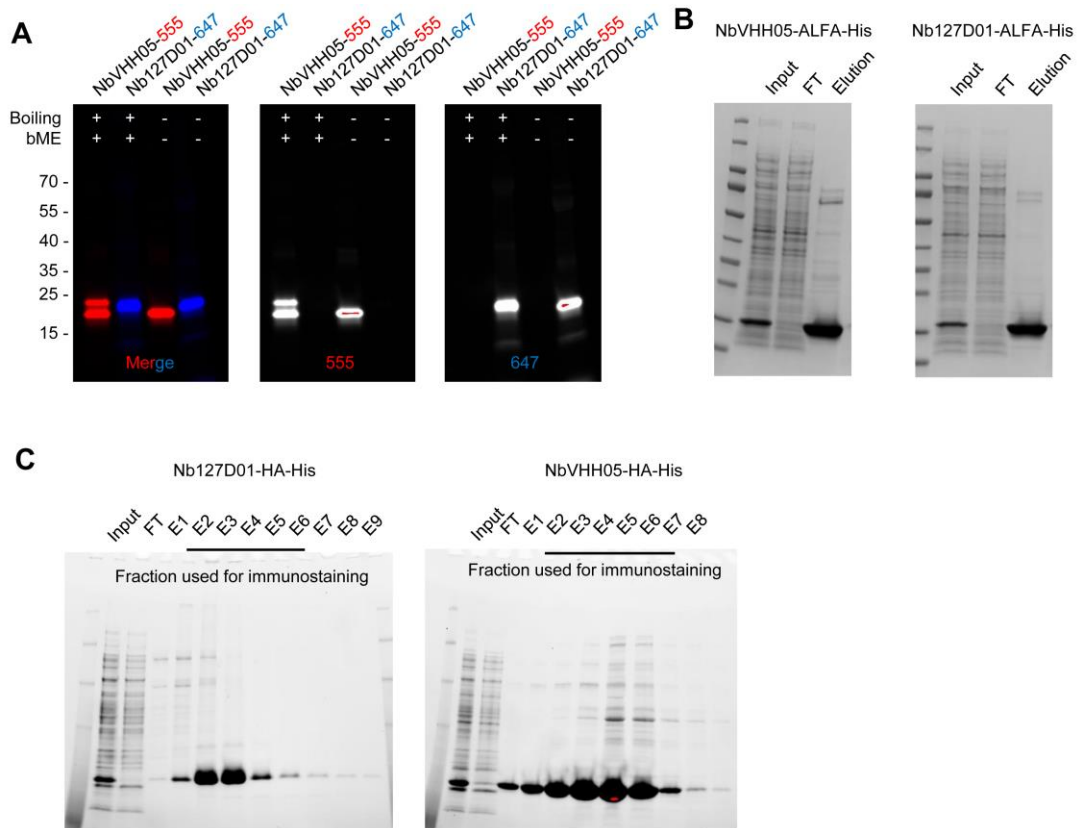


1

2 **Figure 1—figure supplement 2.** Schematic representation of the constructs and
 3 confocal images in S2R+ cells. **(A and B)** Transcriptional elements promoter and SV40
 4 of the expression vectors, the different protein coding modules are represented as
 5 colored filled boxes. **(C and D)** Individual transfection results of VHH05 and 127D01

1 vectors in S2R+ cells. Confocal images show the distribution of fluorescent proteins in
2 the cell. (E) Confocal images of co-transfection of NbVHH05-GFP with different cell
3 compartments mCherry-VHH05 vectors showed the co-localization signal of GFP and
4 mCherry. (F) Confocal images of co-transfection of Nb127D01-GFP with different cell
5 compartments. mCherry-127D01 vectors showed the co-localization signal of GFP and
6 mCherry. (G) Vectors information of NbVHH05-mCherry and mito-GFP-VHH05.
7 Confocal images of co-transfection of these two vectors showed the co-localization
8 signal of GFP and mCherry. (H) Vector information of Nb127D01-mCherry and mito-
9 GFP-127D01. Confocal images of co-transfection of these two vectors showed the co-
10 localization signal of GFP and mCherry.

11



12

13

14

15

16

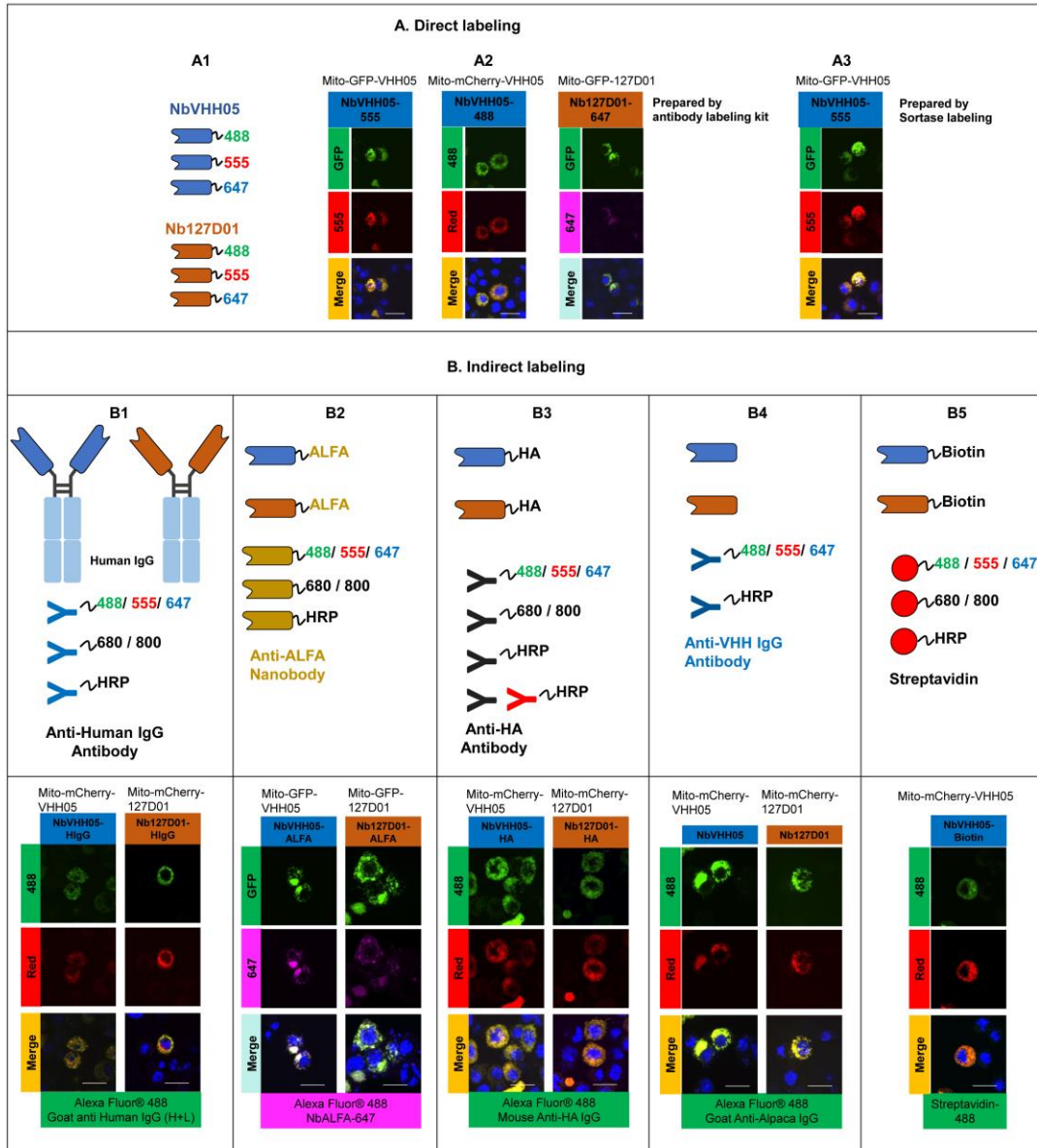
17

18

19

20

Figure 2—figure supplement 1. Nanobody purification and fluorophore-conjugation. (A and B) Coomassie brilliant blue staining of ALFA- and HA-tagged nanobodies using *E. coli* protein expression. (C) Fluorescence signals results of fluor-conjugated nanobodies under 555 and 647 channels.

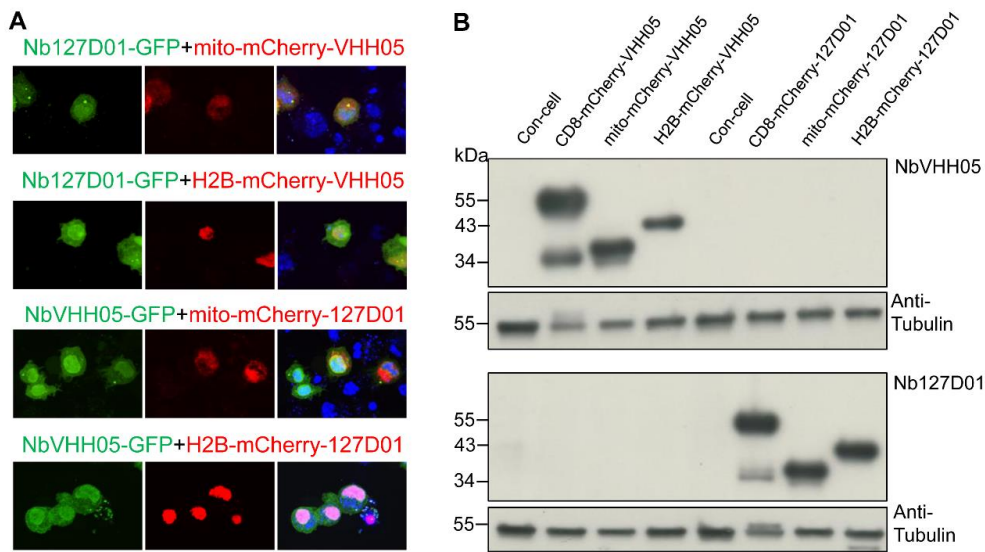


1

2 **Figure 2—figure supplement 2. Different types of NbVHH05 and Nb127D01 and**
 3 **immunofluorescence examples.** (A) Direct labeling can be achieved by linking
 4 purified nanobodies with different fluorophores indirectly by antibody labeling or site-
 5 specifically by sortase-mediated labeling. (A1) Schematics of NbVHH05 and
 6 Nb127D01 with fluorophore-488, 555 or 647. (A2) Confocal images showing direct
 7 immunofluorescence with NbVHH05-555, NbVHH05-488 and Nb127D01-647 in S2R+
 8 cells. (A3) Confocal images showing direct immunofluorescence with NbVHH05-555
 9 prepared by sortase-mediated labeling. (B) Schematics of indirect labeling with
 10 nanobodies containing ALFA-tag, HA-tag, biotin or human IgG as primary antibodies
 11 and confocal images in S2R+ cells. (B1) NbVHH05 and Nb127D01 detected with anti-
 12 VHH IgG antibody. (B2) NbVHH05 and Nb127D01 with ALFA-tag detected by NbALFA.
 13 (B3) NbVHH05 and Nb127D01 with HA-tag detected by anti-HA antibody. (B4)
 14 NbVHH05 and Nb127D01 with biotin prepared by sortase-mediated labeling detected

1 by streptavidin. (B5) NbVHH05 and Nb127D01 with Human IgG detected by anti-
2 Human IgG antibody. Scale bars: 10 μ m.

3



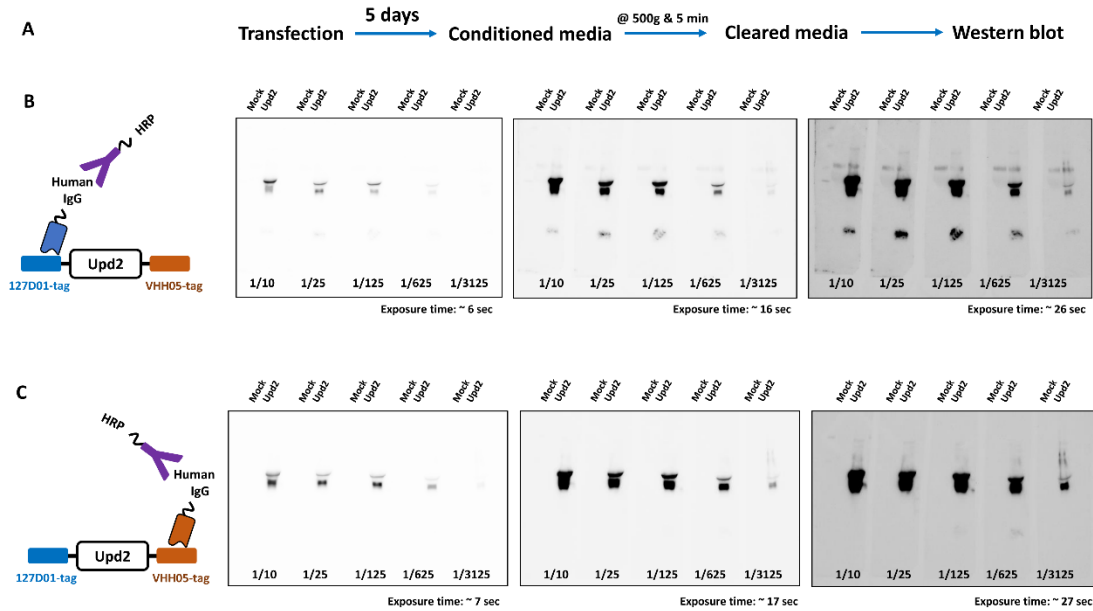
4

5 **Figure 2—figure supplement 3.** Test of potential interaction between VHH05 and
6 127D01. **(A)** Fluorescence confocal results showed no co-localization signal. Co-
7 transfected of Nb127D01-GFP and mito-mCherry-VHH05 or H2B-mCherry-VHH05,
8 NbVHH05-GFP and mito-mCherry-127D01 or H2B-mCherry-127D01 in S2R+ cells. **(B)**
9 Western blots indicate no cross interaction between the two systems. Lysates from
10 S2R+ cells transfected with different types tagged vectors (as in Figure 1) or a mock
11 control plasmid were analyzed by SDS-PAGE and western blotting. The blot was
12 developed with NbVHH05-ALFA and Nb127D01-ALFA, followed by NbALFA-HRP or
13 a mouse anti-tubulin primary antibody, and followed by anti-Mouse IgG HRP.

14

15 **Figure 3—figure supplement 1.** Test of nanobody concentration gradient. Lysates
16 from S2R+ cells transfected with H2B-mCherry-VHH05 or H2B-mCherry-127D01 were
17 analyzed by SDS-PAGE and western blotting. The blot was developed with

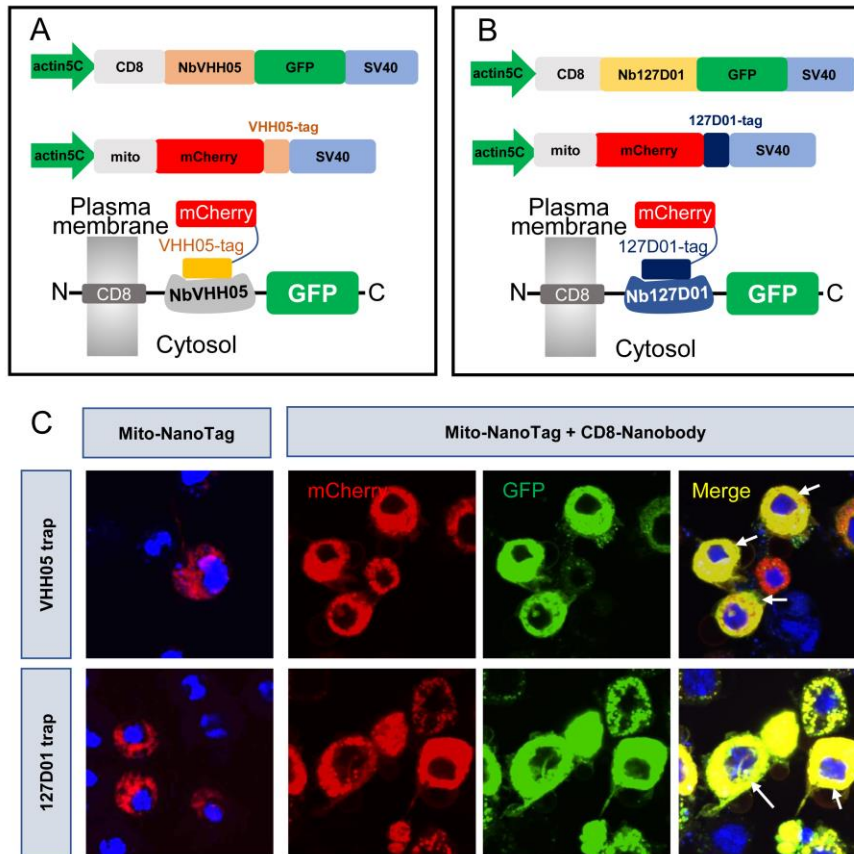
1 NbVHH05-ALFA and Nb127D01-ALFA with a concentration gradient from 1:100,
2 1:1000, 1:10000, 1:100000, followed by NbALFA-HRP or a mouse anti-tubulin primary
3 antibody followed by anti-Mouse IgG HRP. Two conditions of long-time exposure (60
4 s) and short time exposure (20 s) were set for signal reading.
5



6

7 **Figure 3—figure supplement 2. Rapid production of nanobodies in S2 cells for**
8 **western blots.** (A) Workflow production of nanobodies in the fly cell line. (B) Western
9 blot using culture media containing Nb127D01-hlgG, detected by anti-hlgG-HRP. (C)
10 Western blot using culture media containing NbVHH05-hlgG, detected by anti-hlgG-
11 HRP. Five different concentrations and three exposure times were used.

12



1

2

3 **Figure 4—figure supplement 1.** Nanobody-based system for altering localization of

4 NanoTagged proteins. (A and B) Diagram showing the vectors used for cytoplasmic

5 protein trapping. NbVHH05/Nb127D01 is fused to GFP and CD8, and driven by

6 actin5C promoter. Target proteins are mCherry containing VHH05 or 127D01 at the

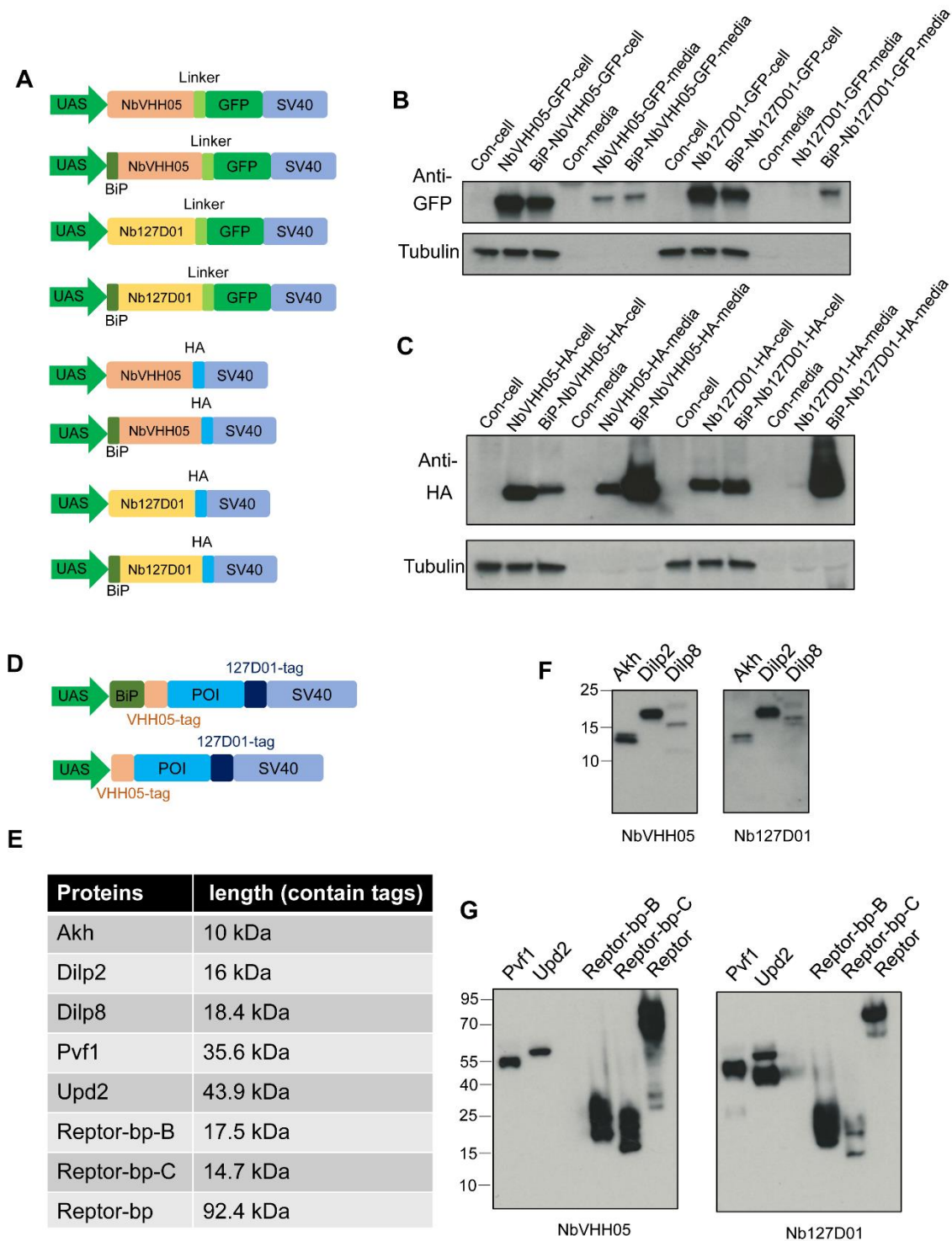
7 C-terminus and mito signal at the N-terminus. (C) Results of transfection of mito-

8 mCherry-NanoTag or co-transfection of CD8-NbVHH05-GFP/mito-mCherry-VHH05

9 and CD8-Nb127D01-GFP/mito-mCherry-127D01 in S2R+ cells. GFP, mCherry and

merge channels show protein expression levels with antibody staining.

10



1

2

Figure 5—figure supplement 1. Transgenic vector information and test in S2R+

3

cells. **(A)** Series of UAS vectors expressing NbVHH05 and Nb127D01 fused to GFP

4

and HA or containing BiP signal. Transcriptional elements promoter and SV40 of the

5

expression vectors, the different protein coding modules are represented as colored

6

filled boxes. **(B)** Lysates or culture media from S2R+ cells transfected with GFP

7

vectors were analyzed by SDS-PAGE and by western blot. The blot was developed

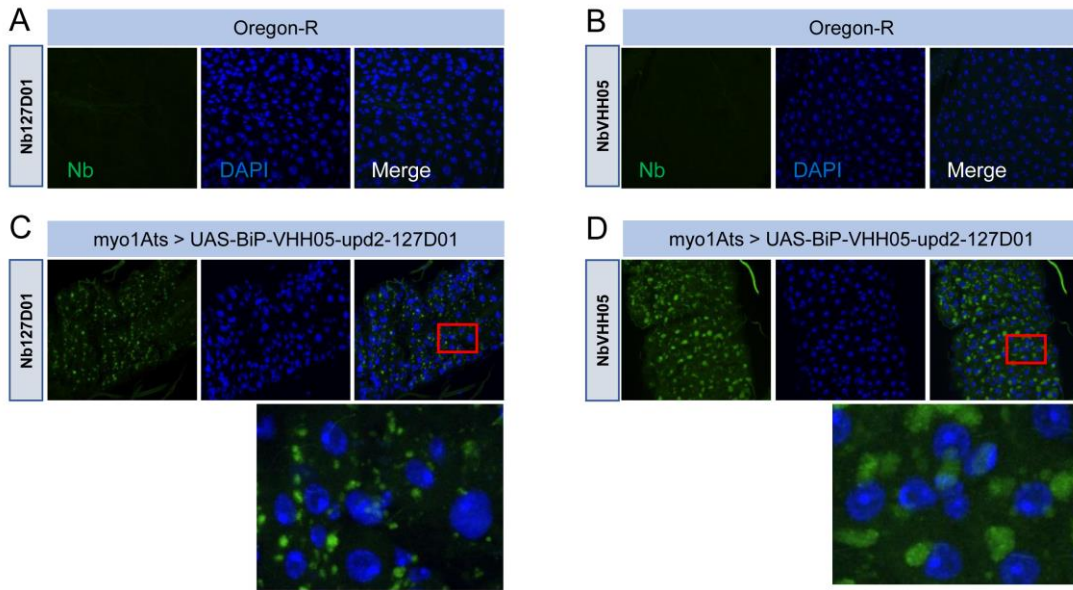
8

with anti-GFP antibody or anti-tubulin antibody. **(C)** Lysates or culture media from

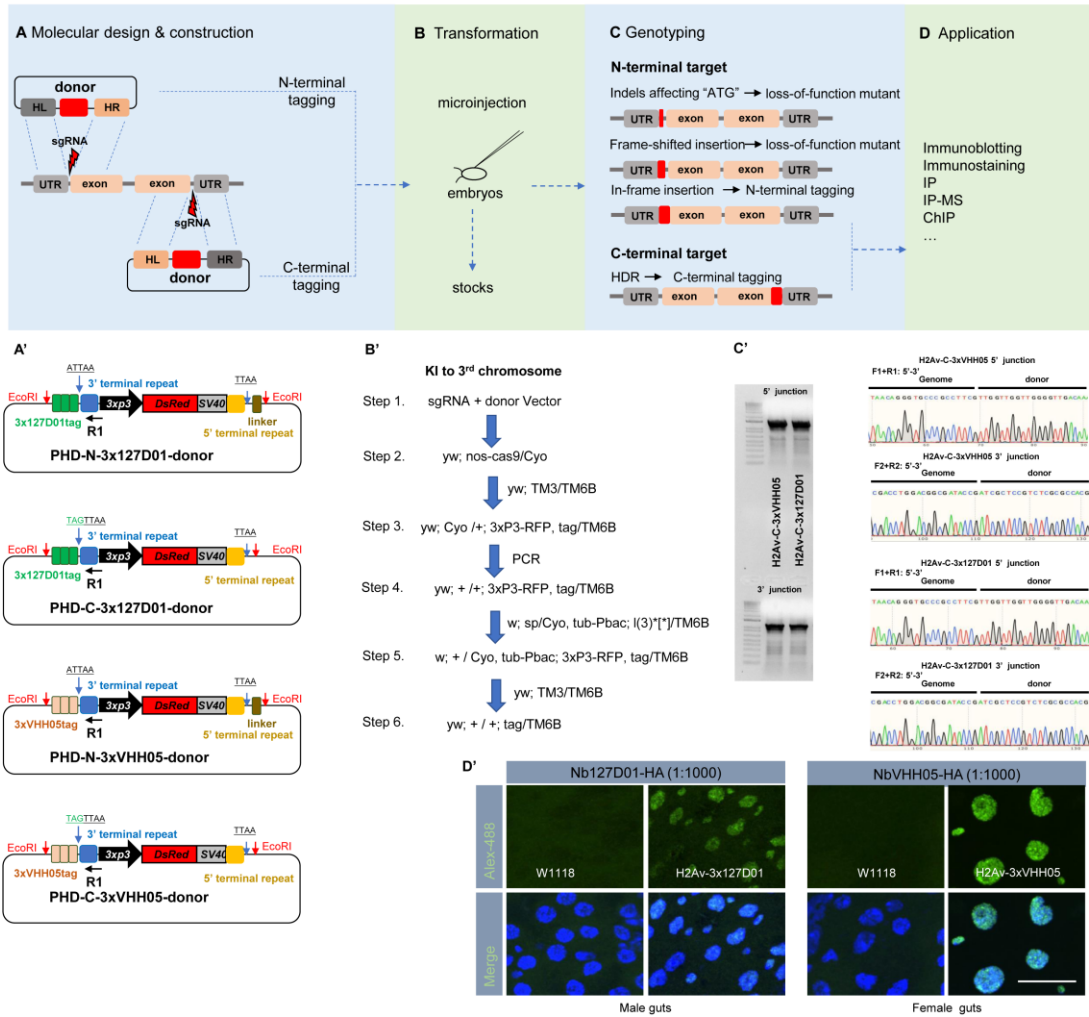
9

S2R+ cells transfected with HA vectors were analyzed by SDS-PAGE and by

1 western blot. The blot was developed with anti-HA antibody or anti-tubulin antibody.
2 (D) Two types of UAS vectors for overexpressing NanoTag labeled genes. N-, C-
3 terminal of POI contains VHH05 and 127D01. BiP is the signal for labeling secreted
4 proteins. (E) Five secreted proteins and three cytoplasm proteins were labeled, and
5 their sizes are indicated. (F) Western blot results of three small size secreted
6 proteins, Akh and Dilp8 showed multiple bands, and Dilp2 only showed a single
7 band. (G) Western blot results of Pvf1, Upd2, REPTOR-bp-B, REPTOR-bp-C,
8 REPTOR-bp-B. The blot was developed with NbVHH05-ALFA and Nb127D01-ALFA
9 followed by NbALFA-HRP in F and G.
10
11

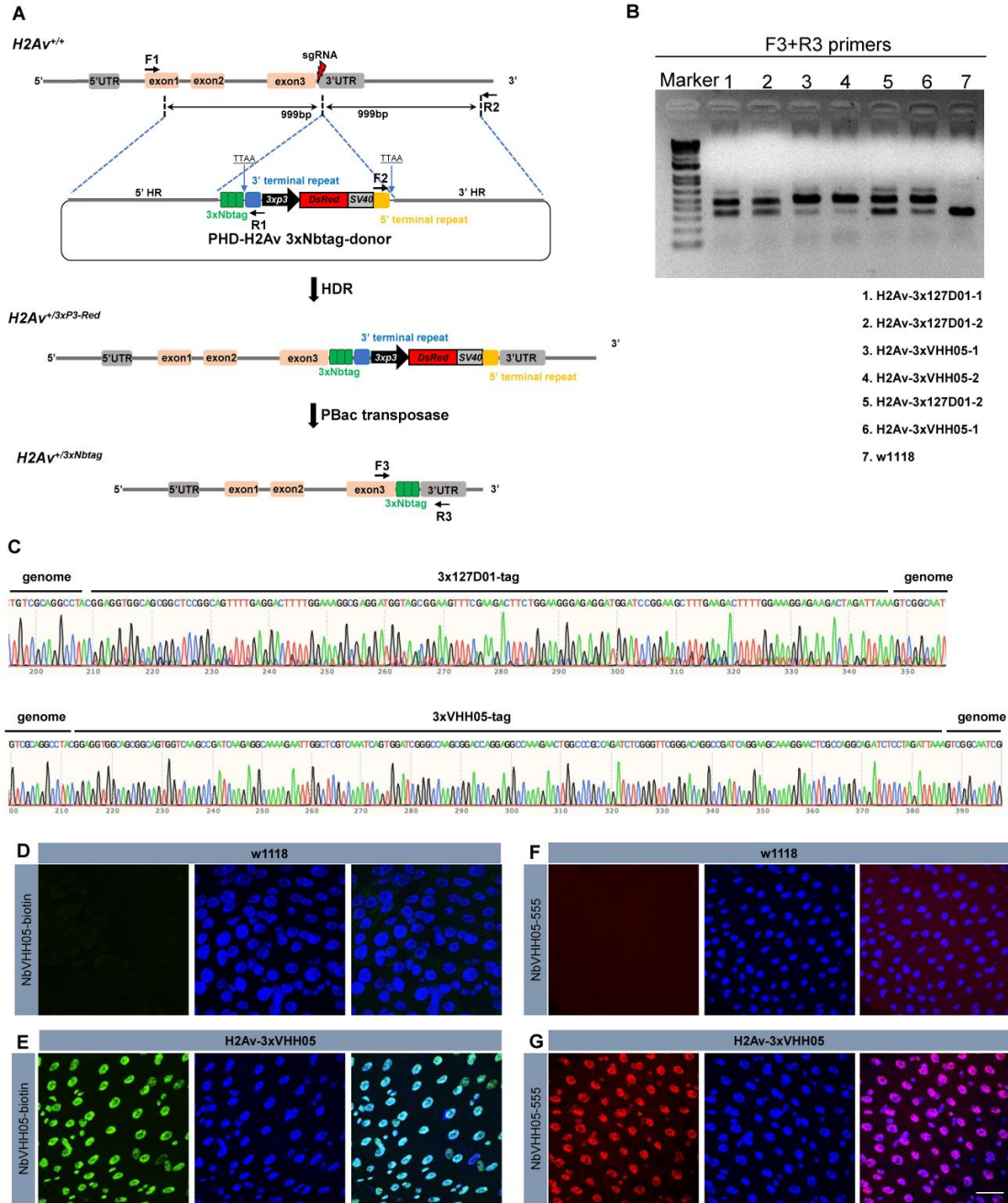


12
13
14 **Figure 5—figure supplement 2.** Immunostaining of double NanoTag-labeled
15 proteins. (A and B) are control Oregon-R flies stained with NbVHH05 and
16 Nb127D01. (C and D) are stained with NbVHH05 and Nb127D01 in the gut of flies
17 carrying *UAS-BiP-VHH05-Upd2-127D01* driven by *Myo1A^{ts}*. Red box indicates an
18 enlarged area of the gut.



1
2
3
4
5
6
7
8
9
10
11
12
13
14

Figure 6—figure supplement 1. Endogenous VHH05- or 127D01-tagging using CRISPR/Cas9. Workflow (A), fly embryos transformation (B), genotyping (C), and applications (D). (A') Common scarless vectors used for constructing donors. N-terminal vectors (PHD-N-3x127D01-donor or PHD-N-3xVHH05-donor) and C-terminal vectors (PHD-C-3x127D01-donor or PHD-C-3xVHH05-donor) contain EcoRI restriction enzyme sites that introduce the homologous arm sequences into donors. (B') Workflow example for introducing knock-in (KI) tags into the third chromosome. (C') Genotyping example of KI 3xVHH05 and 3x127D01 into the C-terminus of H2Av. Gel results showing the 5' and 3' PCR junctions. Representative sequencing chromatogram of PCR products from the junction PCR. (D') Immunostaining of H2Av-3x127D01 and H2Av-3xVHH05. Adult male or female guts were dissected and stained with Nb127D01-HA or NbVHH05-HA. Scale bars: 20 μ m.



1
 2 **Figure 6—figure supplement 2.** Schematic representation of the CRISPR/Cas9-
 3 mediated gene Knock-In approach and the targeted integration of transgene
 4 constructs. (A) Schematic representation of the *H2Av* gene and the sgRNA targeting
 5 site. The thin gray line represents the *H2Av* genomic locus, with open boxes indicating
 6 the promoter, exons, and poly(A) signal. A 164-bp fragment (gray box) located at the
 7 5' end represents the 5' UTR. The two 79-bp, 119-bp and 233-bp fragments (pink
 8 boxes) are exon 1, exon 2 and exon 3, respectively. A 322-bp fragment (gray box)
 9 located at the 3' end is the poly(A) signal. The red lightning icon indicates the sgRNA
 10 site. In the PHD donor construct, the DsRed2 marker expression cassette is driven by
 11 the eye specific 3xP3 promoter. DNA fragments of 999 bp and 999 bp at the 5' and 3'
 12 ends were PCR-amplified, subcloned into vectors, and used as homology arms (5' HR
 13 and 3' HR, respectively). The 3xtag sequence is shown in the green box. 3' terminal

1 repeat and 5' terminal repeats are the piggyBac transposase recognition sequences.
 2 Primer positions for amplification analysis of the integrated insertions in transformed
 3 flies are shown by arrows. Primer pairs of F1/R1 and F2/R2 were used to amplify the
 4 5'- and 3'-end insertion junctions, respectively. The donor plasmid and sgRNA were
 5 injected into the embryos and the donors integrated into the genome. Positive
 6 individuals were screened for red fluorescence of the eye. The selection marker was
 7 removed by crossing with flies expressing the transposase. Primer pairs of F3/R3 were
 8 used to amplify the final insertion. **(B)** PCR amplification was used to confirm the
 9 insertions. Two *H2Av-3x127D01*, four *H2Av-3xVHH05* heterozygous and *w1118*
 10 genome DNA were used as template and the thick gel bands showed the corrected
 11 insertion. **(C)** Sequencing results of the integrated diagnostic DNA fragments
 12 showing 3xtag genome–donor integration. **(D and E)** Indirect immunostaining of *H2Av-*
 13 *3xVHH05* flies. Adult female guts were dissected and stained with NbVHH05-biotin
 14 and visualized by Streptavidin-488. **(F and G)** Direct immunostaining of *H2Av-*
 15 *3xVHH05* flies. Adult female guts were dissected and stained with NbVHH05-555. A
 16 and C were *w1118*, B and D are *H2Av-3xVHH05*. Scale bars: 20 μ m.

17
 18
 19
 20

Table S1. Primers used in this study.

Name	Sequence	Purpose
VHH05-HA-F	TGAATAGGGAATTGGGAATTC AAAATGCAGGTGCAGCTGCA GGAGT	Cloning VHH05-HA PCR fragment to make pW10- UAS-NbVHH05-HA.
VHH05-HA-R	TCAGAACTAGTTTGCTCTAGATTAAGCGTAGTCTGGGACGTC GTATGGGTATGATCCCCACCGCTGCCACCTCCTGAGGAGAC GGTGACCTGG	
127D01-HA-F	GAATAGGGAATTGGGAATTC AAAATGGAGGTTCAATTAGTG GAAT	Cloning 127D01-HA PCR fragment to make pW10- UAS-Nb127D01-HA.
127D01-HA-R	TCAGAACTAGTTTGCTCTAGATTAAGCGTAGTCTGGGACGTC GTATGGGTATGATCCCCACCGCTGCCACCTCCAGAAGAGAC TGTGACCTGC	
VHH05-HA-F	TGAATAGGGAATTGGGAATTC AAAATGCAGGTGCAGCTGCA GGAGT	Cloning VHH05 PCR fragment to make pW10- UAS-NbVHH05-GFP.
Linker-R:	TGATCCCCACCGCTGCCAC	
GFP-Nb-F	GTGGCAGCGGTGGGGATCAGTGAGCAAGGGCGAGGAGCT	Cloning GFP PCR fragment to make pW10-UAS- NbVHH05-GFP or pW10- UAS-Nb127D01-GFP.
GFP-Nb-R	AGATCAGAACTAGTTTGCTCTAGATTACTTGACAGCTCGTCC A	
127d01-HA-F	GAATAGGGAATTGGGAATTC AAAATGGAGGTTCAATTAGTG GAAT	Cloning 127D01 PCR fragment to make pW10- UAS-Nb127D01-GFP.
Linker-R	TGATCCCCACCGCTGCCAC	
BiP-VHH05-HA-F	TGAATAGGGAATTGGGAATTC AAAATGAAGTTATGCATATTA CTGGCCGTCGTGGCCTTTGTTGGCCTCTCGCTCGGGCAGGT	Cloning BiP-VHH05-HA PCR fragment to make

	GCAGCTGCAGGAGT	pW10-BiP-UAS-BiP-NbVHH05-HA.
VHH05-HA-R	TCAGAACTAGTTTGCTCTAGATTAAGCGTAGTCTGGGACGTC GTATGGGTATGATCCCCACCGCTGCCACCTCCTGAGGAGAC GGTGACCTGG	
BiP-127D01-HA-F	TGAATAGGGAATTGGGAATCCAAAATGAAGTTATGCATATTA CTGGCCGTCGTGGCCTTTGTTGGCCTCTCGCTCGGGGAGGT TCAATTAGTGGAAT	Cloning BiP-127D01-HA PCR fragment to make pW10-UAS-BiP-Nb127D01- HA.
127D01-HA-R	TCAGAACTAGTTTGCTCTAGATTAAGCGTAGTCTGGGACGTC GTATGGGTATGATCCCCACCGCTGCCACCTCCAGAAGAGAC TGTGACCTGC	
BiP-VHH05-HA-F	TGAATAGGGAATTGGGAATCCAAAATGAAGTTATGCATATTA CTGGCCGTCGTGGCCTTTGTTGGCCTCTCGCTCGGGCAGGT GCAGCTGCAGGAGT	Cloning BiP-VHH05-GFP PCR fragment to make pW10-BiP-UAS-BiP- NbVHH05-GFP.
GFP-Nb-R	AGATCAGAACTAGTTTGCTCTAGATTACTTGTACAGCTCGTCC A	
BiP-127D01-HA-F	TGAATAGGGAATTGGGAATCCAAAATGAAGTTATGCATATTA CTGGCCGTCGTGGCCTTTGTTGGCCTCTCGCTCGGGGAGGT TCAATTAGTGGAAT	Cloning BiP-127D01-GFP PCR fragment to make pW10-UAS-BiP-Nb127D01- GFP.
GFP-Nb-R	AGATCAGAACTAGTTTGCTCTAGATTACTTGTACAGCTCGTCC A	
pWalium-Colony-F	AGCGCAGCTGAACAAGCTA	Colony PCR for all pWalium 10 insertion.
pWalium-Colony-R	TTTGCAATCTGTAAGCATAAGCA	
pAW-nb-F	TACCATCCAGCCTCCGGACTCTAGAGAATTGGGAATCCAAA ATG	Cloning VHH05-GFP or 127D01-GFP PCR fragments to make pAW- NbVHH05-GFP or pAW- Nb127D01-GFP.
pAW-nb-R	TCCTTCACAAAGATCCTGCTAGCTTACTTGTACAGCTCGTCCA	
pAW-nb-F	TACCATCCAGCCTCCGGACTCTAGA GAATTGGGAATCCAAAATG	Cloning VHH05 or 127D01 PCR fragments to make pAW-NbVHH05-mCherry or pAW-Nb127D01-mCherry.
linker-R	TGATCCCCACCGCTGCCAC	
mCherry-F	GTGGCAGCGGTGGGGGATCAatggtgagcaagggcgagga	Cloning mCherry fragment to make pAW-NbVHH05- mCherry or pAW- Nb127D01-mCherry.
mCherry-R	GTTCTTCACAAAGATCCTGCTAGCTCAcagctcgtcctctcgctaccct tgtacagctcgtccatgc	
H2B-mCherry-F	TACCATCCAGCCTCCGGACTCTAGAatggtccgaaaactagtgg	Cloning H2B-mCherry- VHH05 fragment to make pAW-H2B-mCherry-VHH05.
VHH05-H2B-R	TCCTTCACAAAGATCCTGCTAGCTCAGGAAATCTGCCGTGCC AATTCTTAGCCTCTTGATCTGCCTGtccggatccctgtacagctgtcca tgc	
H2B-mCherry-F	TACCATCCAGCCTCCGGACTCTAGAatggtccgaaaactagtgg	Cloning H2B-mCherry- 127D01 fragment to make pAW-H2B-mCherry-
127D01-H2B-R	TCCTTCACAAAGATCCTGCTAGCTCAATCCTCGCCTTTCCAGA AATCTTCAAACCTtccggatccctgtacagctcgtccatgc	

		127D01.
CD8-mCherry-F	TACCATCCAGCCTCCGGACTCTAGAatggcctcaccgttgaccgg	Cloning CD8-mCherry-VHH05 fragment to make pAW-CD8-mCherry-VHH05.
VHH05-H2B-R	TCCTTCACAAAGATCCTGCTAGCTCAGGAAATCTGCCGTGCC AATTCTTTAGCCTCTTGATCTGCCTGtccggatccctgtacagctcgtcca tgc	
CD8-mCherry-F	TACCATCCAGCCTCCGGACTCTAGAatggcctcaccgttgaccgg	Cloning CD8-mCherry-127D01 fragment to make pAW-CD8-mCherry-127D01.
127D01-H2B-R	TCCTTCACAAAGATCCTGCTAGCTCAATCCTCGCCTTTCCAGA AATCTTCAAACCTtccggatccctgtacagctcgtccatgc	
mito-mCherry-F	TACCATCCAGCCTCCGGACTCTAGAatgagtctgactccagttc	Cloning mito-mCherry-VHH05 fragment to make pAW-mito-mCherry-VHH05.
VHH05-H2B-R	TCCTTCACAAAGATCCTGCTAGCTCAGGAAATCTGCCGTGCC AATTCTTTAGCCTCTTGATCTGCCTGtccggatccctgtacagctcgtcca tgc	
mito-mCherry-F	TACCATCCAGCCTCCGGACTCTAGAatgagtctgactccagttc	Cloning mito-mCherry-127D01 fragment to make pAW-mito-mCherry-127D01.
127D01-H2B-R	TCCTTCACAAAGATCCTGCTAGCTCAATCCTCGCCTTTCCAGA AATCTTCAAACCTtccggatccctgtacagctcgtccatgc	
mCherry-VHH05-F	ctctcatctgtaccacagcggatccggaCAGGCAGATCAAGAGGCTAAAG AATTGGCAGGCAGATTTCCggatccggaatggtgagcaagggcgagga	Cloning VHH05-mCherry fragment to make pAW-CD8-VHH05-mCherry.
mCherry-VHH05-R	GTTCTTCACAAAGATCCTGCTAGCTCActgtacagctcgtccatgc	
mCherry-127D01-F	ctctcatctgtaccacagcggatccggaAGTTTTGAAGATTTCTGGAAAGG CGAGGATggatccggaatggtgagcaagggcgagga	Cloning 127D01-mCherry fragment to make pAW-CD8-127D01-mCherry.
mCherry-VHH05-R	GTTCTTCACAAAGATCCTGCTAGCTCActgtacagctcgtccatgc	
AR205-GFP-127D01 1X	AACGGCATCAAGGTGAACCTCAAGATCCGCCACAACATCGAG GACGGCAGCGTGCAGCTCGCCGACCACTACCAGCAGAACAC CCCCATCGGCGACGGCCCCGTGCTGCTGCCGACAACCACT ACCTGAGCACCCAGTCCGCCCTGAGCAAAGACCCCAACGAG AAGCGGATCACATGGTCCTGCTGGAGTTCGTGACCGCCGC CGGGATCACTCTCGGCATGGACGAGCTGTACAAGGGCTCCG GCAGTTTTGAGGACTTTTTGAAAGGCGAGGATTAGGGTTCCG GTGGATCCGGA	Cloning synthesized GFP fragment with 1x127D01 tag to make pAW-HGP-BiP-GFP-1x127D01.
AR206-GFP-127D01 2X	AACGGCATCAAGGTGAACCTCAAGATCCGCCACAACATCGAG GACGGCAGCGTGCAGCTCGCCGACCACTACCAGCAGAACAC CCCCATCGGCGACGGCCCCGTGCTGCTGCCGACAACCACT ACCTGAGCACCCAGTCCGCCCTGAGCAAAGACCCCAACGAG AAGCGGATCACATGGTCCTGCTGGAGTTCGTGACCGCCGC CGGGATCACTCTCGGCATGGACGAGCTGTACAAGGGCTCCG GCAGTTTTGAGGACTTTTTGAAAGGCGAGGATTAGGGTTCCG GTTTCGAAGACTTCTGGAAGGGAGAGGATTAGGGTTCCGGTG GATCCGGA	Cloning synthesized GFP fragment with 2x127D01 tag to make pAW-HGP-BiP-GFP-2x127D01.

AR207-GFP-127D01 3X	AACGGCATCAAGGTGAACTTCAAGATCCGCCACAACATCGAG GACGGCAGCGTGCAGCTCGCCGACCACTACCAGCAGAACAC CCCCATCGGCGACGGCCCCGTGCTGCTGCCCGACAACCACT ACCTGAGCACCCAGTCCGCCCTGAGCAAAGACCCCAACGAG AAGCGCGATCACATGGTCCTGCTGGAGTTCGTGACCGCCGC CGGGATCACTCTCGGCATGGACGAGCTGTACAAGGGCTCCG GCAGTTTTGAGGACTTTTTGAAAGGCGAGGATGGTAGCGGAA GTTTCGAAGACTTCTGGAAGGGAGAGGATGGCTCCGGAAGC TTTGAAGACTTTTTGAAAGGAGAAGACTAGGGTTCCGGTGGA TCCGGA	Cloning synthesized GFP fragment with 3x127D01 tag to make pAW-HGP-BiP-GFP-3x127D01.
AR208-GFP-VHH05 1X	AACGGCATCAAGGTGAACTTCAAGATCCGCCACAACATCGAG GACGGCAGCGTGCAGCTCGCCGACCACTACCAGCAGAACAC CCCCATCGGCGACGGCCCCGTGCTGCTGCCCGACAACCACT ACCTGAGCACCCAGTCCGCCCTGAGCAAAGACCCCAACGAG AAGCGCGATCACATGGTCCTGCTGGAGTTCGTGACCGCCGC CGGGATCACTCTCGGCATGGACGAGCTGTACAAGGGCAGTG GTCAAGCCGATCAAGAGGCAAAGAATTGGCTCGTCAAATCA GTTAGGGTTCCGGTGGATCCGGA	Cloning synthesized GFP fragment with 1xVHH05 tag to make pAW-HGP-BiP-GFP-1xVHH05.
AR209-GFP-VHH05 2X	AACGGCATCAAGGTGAACTTCAAGATCCGCCACAACATCGAG GACGGCAGCGTGCAGCTCGCCGACCACTACCAGCAGAACAC CCCCATCGGCGACGGCCCCGTGCTGCTGCCCGACAACCACT ACCTGAGCACCCAGTCCGCCCTGAGCAAAGACCCCAACGAG AAGCGCGATCACATGGTCCTGCTGGAGTTCGTGACCGCCGC CGGGATCACTCTCGGCATGGACGAGCTGTACAAGGGCAGTG GTCAAGCCGATCAAGAGGCAAAGAATTGGCTCGTCAAATCA GTGGATCGGGCCAAGCGGACCAGGAGGCCAAAGAAGTGGCC CGCCAGATCTCGTAGGGTTCCGGTGGATCCGGA	Cloning synthesized GFP fragment with 2xVHH05 tag to make pAW-HGP-BiP-GFP-2xVHH05.
AR210-GFP-VHH05 3X	AACGGCATCAAGGTGAACTTCAAGATCCGCCACAACATCGAG GACGGCAGCGTGCAGCTCGCCGACCACTACCAGCAGAACAC CCCCATCGGCGACGGCCCCGTGCTGCTGCCCGACAACCACT ACCTGAGCACCCAGTCCGCCCTGAGCAAAGACCCCAACGAG AAGCGCGATCACATGGTCCTGCTGGAGTTCGTGACCGCCGC CGGGATCACTCTCGGCATGGACGAGCTGTACAAGGGCAGTG GTCAAGCCGATCAAGAGGCAAAGAATTGGCTCGTCAAATCA GTGGATCGGGCCAAGCGGACCAGGAGGCCAAAGAAGTGGCC CGCCAGATCTCGGGTTCCGGACAGGCCGATCAGGAAGCAA GAACTCGCCAGGCAGATCTCTAGGGTTCCGGTGGATCCG GA	Cloning synthesized GFP fragment with 3xVHH05 tag to make pAW-HGP-BiP-GFP-3xVHH05.
AR211-Cloning Twist gBlock R	TCCGGATCCACCGGAACC	Cloning GFP fragment to make pAW-HGP-BiP-GFP-VHH05, pAW-HGP-BiP-GFP-2xVHH05, pAW-HGP-BiP-GFP-3xVHH05, pAW-HGP-BiP-GFP-127D01,
AR212-Cloning Twist gBlock F	AACGGCATCAAGGTGAACTTCAAG	
AR213-Cloning GFP internal R	CTTGAAGTTCACCTTGATGCCGTTCTTCTGCTTGTCGGCCATG A	

		pAW-BiP-HGP-GFP-2x127D01, pAW-HGP-BiP-GFP-3x127D01.
AR345-BiP Fw	AGCCTCCGGACTCTAGAAACATGAAGTTATGCATATTACTGGC CGTCG	Cloning NbVHH05/Nb127D01 and human IgG PCR fragments to make pMT-HGP-v3-Nb127D01-hlgG and pMT-HGP-v3-NbVHH05-hlgG.
AR346-hlgG Fw	GGCGGAGGTGGCTCTGGTGG	
AR347-hlgG Rv	TTTCTCCGGATCCACCGGAACCTTCCCTGGACTTAATGACA ATGA	
AR349-127D01 Rv	CCACCAGAGCCACCTCCGCCAGAAGAGACTGTGACCTGCGT	
AR348-VHH05 Rv	CCACCAGAGCCACCTCCGCTGAGGAGACGGTGACCTGGG	
AR184_pET-26b0-VHH05-Fw	TCTGTGGGTCTCGGATGGCCAGGTGCAGCTGCAGGAGTC	Cloning NbVHH05 PCR fragment to make pET-26b-Nb127D01-ALFA-His.
AR185_pET-26b0-VHH05-Rv	TCTGTGGGTCTCCAGCCTGAGGAGACGGTGACCTGGG	
AR186_pET-26b-127D01-Fw	TCTGTGGGTCTCGGATGGCCAGGTTCAATTAGTGAATCTG GCGG	Cloning Nb127D01 PCR fragment to make pET-26b-Nb127D01-ALFA-His.
AR187_pET-26b-127D01-Rv	TCTGTGGGTCTCCAGCCAGAAGAGACTGTGACCTGCGTTC	
AR352-PelB	gctgccagccggcgatggc	Cloning NbVHH05/Nb127D01 to make pET-26b-Nb127D01-HA-His and pET-26b-NbVHH05-HA-His.
AR343-127D01 HA Rv	GTGGTGGTGGTGGTGGTgcccagagccggcgtaacaggcacgtcatagg ggtagccagagccAGAAGAGACTGTGACCTGCGTTC	
AR344-VHH05-HA Rv	GTGGTGGTGGTGGTGGTgcccagagccggcgtaacaggcacgtcatagg ggtagccagagccTGAGGAGACGGTGACCTGGGT	
pAW-nb-F	TACCATCCAGCCTCCGGACTCTAGA GAATTGGGAATTCCAAAATG	Cloning BiP-NbVHH05 or BiP-Nb127D01 fragments to make pAW-BiP-NbVHH05-mCherry-KDEL and pAW-BiP-Nb127D01-mCherry-KDEL.
linker-R	TGATCCCCCACCCTGCCAC	
mCherry-KDEL-F	GTGGCAGCGGTGGGGATCAatggtgagcaagggcgagga	Cloning mCherry-KDEL fragment to make pAW-BiP-NbVHH05-mCherry-KDEL and pAW-BiP-Nb127D01-mCherry-KDEL.
mCherry-KDEL-R	GTTCTTCACAAAGATCCTGCTAGCTCAcagctcgtcctctcgctaccct tgtacagctgctcatgc	
VHH05-GFP-F	tctgctaccacagcgctagcATGCAGGTGCAGCTGCAGGA	Cloning NbVHH05-GFP fragment to make pAW-CD8-NbVHH05-GFP.
pAW-nb-R	TCCTTCACAAAGATCCTGCTAGC TTACTTGTACAGCTCGTCCA	
127-GFP-F	tctgctaccacagcgctagcATGGAGGTTCAATTAGTGGA	Cloning Nb127D01-GFP fragment to make pAW-CD8-Nb127D01-GFP.
pAW-nb-R	TCCTTCACAAAGATCCTGCTAGC TTACTTGTACAGCTCGTCCA	
CD8-mCherry-F	TACCATCCAGCCTCCGGACTCTAGAatggcctcaccgttgaccgg	Cloning CD8 fragment to make pAW-CD8-NbVHH05-
CD8-m-nb-R:	gctagcgtgtggtagcaga	

		GFP or pAW-CD8-Nb127D01-GFP.
BiP-VHH05/127tag-F	GAATTCAAAATGAAGTTATGCATATTACTGGCCGTCGTGGCC TTTGTGGCCTCTCGCTCGGGTCCCAGGCAGATCAAGAGGCT AAAGAATTGG	Cloning BiP-127D01-VHH05 fragment to make pW10-UAS-BiP-127D01-VHH05.
BiP-VHH05/127tag-R	TCAATCCTCGCCTTTCCAGAAATCTTCAAACCTTGATCCCCA CCAGATCTGCTGCCACCTCCGAAATCTGCCGTGCCAATTCT TTAGCCTCTT	
Akh-V127-F	AGATTTCCGGAGGTGGCAGCCAATTGACCTTCTCGCCGGA	Cloning Akh fragment to make pW10-UAS-BiP-VHH05-Akh-127D01.
Akh-V127-R	TCAAACCTTGATCCCCACCTCGCGGTGCTTGCAGTCCA	
Dilp2-V127-F	AGATTTCCGGAGGTGGCAGCACGCTCTGCAGTAAAAGCT	Cloning Dilp2 fragment to make pW10-UAS-BiP-VHH05-Dilp2-127D01.
Dilp2-V127-R	TCAAACCTTGATCCCCACCATTTCTGACCACGGAGCAGT	
Dilp8-V127-F	AGATTTCCGGAGGTGGCAGCAGCTTCTGCTCCCTGGAGCGG A	Cloning Dilp2 fragment to make pW10-UAS-BiP-VHH05-Dilp8-127D01.
Dilp8-V127-R	TCAAACCTTGATCCCCACCGCAGAAGAACTCCTCCTCGCA	
Pvf1-V127-F	AGATTTCCGGAGGTGGCAGCGGCTCCTTGGTGTCCCCGAAC AACA	Cloning Pvf1 fragment to make pW10-UAS-BiP-VHH05-Pvf1-127D01.
Pvf1-V127-R	TCAAACCTTGATCCCCACCAACTGTACAGGGTGGTGTTA	
Upd2-V127-F	AGATTTCCGGAGGTGGCAGCGCGACACTTGCAGCACCAG GT	Cloning Upd2 fragment to make pW10-UAS-BiP-VHH05-Upd2-127D01.
Upd2-V127-R	TCAAACCTTGATCCCCACCACTCATTGGATCCGCCATCG	
Reptor-bpb-V127-F	ACTCTGAATAGGGAATTGGGAATTCAAAATGCAGGCAGATC AAGAGGCTAAAGAATTGGCACGGCAGATTTCCggatccggaGCT AGCATGGCTGATATGGAGATACA	Cloning REPTOR-bp-B or REPTOR-bp-C fragments to make pW10-UAS-127D01-REPTOR-bp-B-VHH05, pW10-UAS-127D01-REPTOR-bp-C-VHH05.
Reptor-bpb-V127-R	CAAACCTTGATCCCCACCACTCATTGGATCCGCCATCG GA	
Reptor-V-F	GCAGATTTCCggatccggaGCTAGCATGACAGAGAATCAGCTGTA TCCC	Cloning REPTOR fragment to make pW10-UAS-127D01-REPTOR-VHH05.
Reptor-V127-R	TCAAACCTTGATCCCCACCCGACGATTTACGCAGCTCCTCG AG	
pHD-N-3X127-tag-F	AATTGAATTTAGCGGCCGGAATTCATGAGTTTTGAGGACTTT TGGA	Cloning 3X127D01 fragment to make pScarlessHD-N-3x127D01-DsRed.
pHD-N-3X127-tag-R	ATTATCTTTCTAGGGTTAATGTCTTCTCCTTTCCAAAAGT	
pHD-N-3x127-3xp3-red-F	ACTTTTGGAAAGGAGAAGACATTAACCCTAGAAAGATAAT	Cloning 3XP3DsRed fragment to make pScarlessHD-N-3x127D01-DsRed.
pHD-N-3x127-3xp3-red-R:	CTAGTCCTGCAGGTTTAAACGAATTCGGAACCTCCTGAACCA CCAG	
pHD-C-3X127-tag-F	AATTGAATTTAGCGGCCGGAATTCGGAGGTGGCAGCGGCT	Cloning 3X127D01

	CCGGC	fragment to make
pHD-C-3X127-tag-R	TAGTCCTGCAGGTTTAAACGAATTCTTAACCCTAGAAAGATAG TC	pScarlessHD-C-3x127D01- DsRed.
pHD-N-3XVHH-tag-F	AATTGAATTTAGCGGCCGCGAATTCATGCAAGCCGATCAAGA GGCAAA	Cloning 3XVHH05 fragment to make pScarlessHD-N- 3xVHH05-DsRed.
pHD-N-3XVHH-tag-R	ATTATCTTTCTAGGGTTAATGGAGATCTGCCTGGCGAGTT	
pHD-N-3xVHH-3xp3- red-F	AACTCGCCAGGCAGATCTCCATTAACCCTAGAAAGATAAT	Cloning 3XP3DsRed fragment to make
pHD-N-3x127-3xp3-red- R:	CTAGTCCTGCAGGTTTAAACGAATTCGGAACCTCCTGAACCA CCAG	pScarlessHD-N-3xVHH05- DsRed.
pHD-C-3XVHH-tag-F	AATTGAATTTAGCGGCCGCGAATTCGGAGGTGGCAGCGGCtG TGGT	Cloning 3XVHH05 fragment to make pScarlessHD-C- 3xVHH05-DsRed.
pHD-C-3X127-tag-R	TAGTCCTGCAGGTTTAAACGAATTCTTAACCCTAGAAAGATAG TC	
H2av-up-F:	TTGGTGGATCTGGAGGTTCTGGTTGGTTGGGGTTGACAA	Cloning upstream fragment of H2Av to make
H2av-up-R:	CCGGAGCCGCTGCCACCTCCGTAGGCCTGCGACAGAATGA	pScarlessHD-C-3xVHH05- H2Av-DsRed or pScarlessHD-C-3x127D01- H2Av-DsRed.
H2av-down-F:	GACTATCTTTCTAGGGTTAAAGTCGGCAATCGGACGCCTT	Cloning downstream fragment of H2Av to make
H2av-down-R:	GTTTAAACGAATTCGCCCTTCGCTCCGTCTCGCGCCACGA	pScarlessHD-C-3xVHH05- H2Av-DsRed or pScarlessHD-C-3x127D01- H2Av-DsRed.
H2av-sg-F:	GTCGCGATTGCCGACTGGGTTAGT	Sense and anti-sense oligo
H2av-sg-R:	AAACACTAACCCAGTCGGCAATCG	for sgRNA plasmid.